INVESTIGATION OF EROSION WEAR OF DUCTILE MATERIALS WITH AND WITHOUT COATING

Thesis Report submitted in partial fulfillment of the requirements for the award of degree of

Master of Engineering
In
PRODUCTION AND INDUSTRIAL ENGINEERING

By:
Rakesh Kumar
(Roll no. 800982021)

Under the supervision of

Mr. Satish Kumar
(Assistant Professor, MED, Thapar University Patiala)

(July 2011)
Mechanical Engineering Department
Thapar University, Patiala-147004

DECLARATION

I hereby declare that the work which is being presented in the dissertation work entitled, **"INVESTIGATION OF EROSION WEAR OF DUCTILE MATERIALS WITH AND WITHOUT COATING"**, in partial fulfillment of the requirements for the award of degree of Master of Engineering in Mechanical Engineering with specialization in **PRODUCTION & INDUSTRIAL ENGINEERING** submitted in Mechanical Engineering Department of Thapar University, Patiala, is an authentic record of my own work carried out under the supervision of **Mr. Satish Kumar** refers other researcher's works which are duly listed in the reference section. The matter presented in this thesis has not been submitted for the award of any other degree of this or any other university.

15/07/11

Rakesh Kumar

This is to certify that the above statement made by the candidate is correct and true to the best of my knowledge.

Mr. Satish Kumar
Assistant Professor
Mechanical Engineering Department
Thapar University, Patiala

Counter signed by

Dr. Ajay Batish
Professor & head
Mechanical Engineering Department
Thapar University, Patiala

Dr. S.K. Mohapatra
Dean Of Academic Affairs
Thapar University,Patiala

ACKNOWLEDGEMENT

This thesis has been an inspiring, very challenging, but always interesting and exciting experience. In first place, I would like to express my sincere gratitude to my guide **Mr. Satish Kumar, Assistant professor, Department of Mechanical Engineering, Thapar University, Patiala** for acting as my thesis supervisor and giving valuable guidance, for the patience, encouragement, many fruitful discussions, and never giving up on me.

It is my proud privilege to express regards and sincere thanks to **Dr. Ajay Batish, Professor and Head, Mechanical Engineering Department, Thapar University, Patiala** for giving me the opportunity of being a member of this project for the complete accomplishment of two years M.E. Course. I heartily thanks to Mr. Purshottam Kumar for his help in conducting the test on S.E.M. machine.

Finally, I thanks to entire faculty and staff of Department of Mechanical Engineering, Thapar University, Patiala for their help, Inspiration and moral support, which went a long way in successfully completion of my thesis.

Rakesh Kumar

Abstract

Wear is one of the most common problems encountered in industries like thermal power plants, hydropower plants, mining industries, food-processing industries etc. in which solid liquid mixture is transported through pumps and pipes. Wear is the loss of material from a component due to a mechanical interaction with another object. Many types of solids, liquids, and even high-velocity gases can remove material and change the physical dimensions and functionality of a part. Corrosion and erosion are the main causes of wear. Corrosion is caused by chemical reaction of material with its environment. Erosion wear is due to exposure to moving liquids and gases, which may or may not contain hard particulate.Effect of erosion wear in slurry pumps and pipes is predominantly more as compared to corrosion. The service life of equipment of slurry transport system is reduced by erosion caused by solid-liquid mixture following through the slurry transport system.

Present work is to study the erosion behaviour of ductile materials. 13Cr4Ni steel taken for the study of erosion wear of pump and piping system with fly ash slurry. To improve the wear resistance of 13Cr4Ni steel , aluminium oxide and chromium oxide powder coatings were done by HVOF thermal spray coating method. The erosion wear evaluated with varying the parameters impact angle, flow rate and time and using jet tester as test apparatus. It is observe that both coatings shows better performance than uncoated steel in all conditions in which erosion wear test was performed. Chromium oxide coating shows the minimum wear among the other aluminium oxide coating and uncoated 13Cr4Ni steel. The maximum erosion wear reported at 30° impact angle and minimum at 90° in both coated and uncoated steel. Cr_2O3 coated steel shows approximately 3 times better performance than uncoated 13Cr4Ni steel. Erosion of uncoated steel under normal impact is due to platelet mechanism but for coatings under similar condition is due to crack formation. Erosion wear of both coated and uncoated steel increases with increase in flow rate and test time duration.

LIST OF CONTENTS

LIST OF FIGURES

LIST OF TABLES

CHAPTER 1

INTRODUCTION

Wear is one of the most common problems encountered in industries like thermal power plants, hydropower plants, mining industries, food processing industries etc. in which solid liquid mixture is transported through pumps and pipes. Wear is the loss of material from a component due to a mechanical interaction with another object. Many types of solids, liquids, and even high-velocity gases can remove material and change the physical dimensions and functionality of a part. Corrosion and erosion are the main causes of wear. Corrosion is caused by chemical reaction of material with its environment. Erosion wear is due to exposure to moving liquids and gases, which may or may not contain hard particulate.Effect of erosion wear in slurry pumps and pipes is predominantly more as compared to the corrosion. The service life of equipment of slurry transport system is reduced by erosion caused by solid-liquid mixture following through the slurry transport system. So slurry erosion is important field should be investigated.

1.1) TYPES OF WEAR:

There are several types and mechanisms of wear. These are:-

1.1.1) Abrasive

1.1.2) Adhesive

1.1.3) Erosion

1.1.4) Corrosive

1.1.5) Fatigue Wear

1.1.1) Abrasive Wear:

Abrasive wear can be defined as the kind of wear that occurs when a hard surface slides or contuse to have relative motion with a softer surface. Hard materials or an asperity that cut groves during this motion produces abrasive wear. These asperities can be those present in the matting surface or any foreign material. This generation of wear fragments hastens the process of wear if not removed.

1.1.2) Adhesive Wear:

Adhesive wear can be defined as the kind of wear that occurs due to localized bonding between the contacting or the mating surfaces. In this kind of wear there is actual transfer of material between the mating surfaces. This transfer depends upon the degree of hardness of the two mating surface. But the precondition for this kind of wear is the intimate contact between the two surfaces. But the application of lubricating surface, oil or grease decreases the tendency of this kind of wear.

1.1.3) Erosive Wear:

This kind of wear is defined as process of metal removal due to impingement of solid particles on a surface. This can also occur due to gas & liquid but the erosion by this medium doesn't carry. There are some specific characteristics of this kind of wear like: -- when the angle of impingement is small, the wear produced is closely analogous to abrasion. When the angle of impingement is normal then material flows by plastic flow or is dislodged by brittle fracture.

1.1.4) Corrosive Wear:

Most metals are thermodynamically unstable in atmosphere & reat with oxygen to form oxides. These oxides form layer or scales over the surface. These scales are very loosely bonded to the surface. They can be easily removed by treating it with acids, gases, alkalis, etc. these kind of wear creates pits 7 gradually harm the metal surface.

1.1.5) Fatigue Wear:

Fatigue Wear or fracture arises when the components is subjected to cyclic compression & tension above a threshold stress. The surface wears down in this process. It starts with the formation of microcraks & it gradually spreads & with repeated loading it actually grows to the surface. Vibration is the common cause of fatigue.

1.2) EROSION WEAR:

Erosion wear is a process of progressive removal of material from a target surface due to repeated impacts of solid particles. The particles suspended in the flow of solid liquid mixture erode the wetted passes limiting the service life of equipment used for slurry transportation system. Erosion wear caused by the kinetic energy transferred to target surface by impinging solid particles. Material loss of target material is higher for higher kinetic energy of impinging particle. So impact velocity largely affects the erosion wear of target material. Also erosion wear

depends on the angle with which erodent strikes at target surface (impact angle), slurry concentration, erodent size, erodent shape etc. the extent of erosion wear changes material to material of target surface.

Erosion wear can be classified into three categories: solid particle erosion, liquid impact erosion and cavitation erosion. Solid particle erosion is the loss of material volume from target material due to continues impingement of solid particles present in the flowing fluid. The continues striking of liquid jet on material surface cause liquid impact erosion. The deformation and removal of material from target surface due to repeated nucleation, growth and blastic collapse of bubbles is known as cavitation.

1.3) MECHANISM OF EROSION WEAR:

To identify the effect of parameters it is necessary to understand the mechanism of material removal due to erosion wear. Erosion wear depends on impact angle, impact velocity, erodent material, carrier fluid, erodent size and shape, and target material. Both ductile and brittle material show different erosion wear mechanism. The erosion wear mechanism are classified as cutting, ploughing and subsurface deformation and cracking.

1.3.1) Cutting Mechanism:

Cutting wear occurs when a hard particle cuts through a soft target material. Cutting mechanism takes place when the impacting particle contacts the target material at positive rack angle and cut

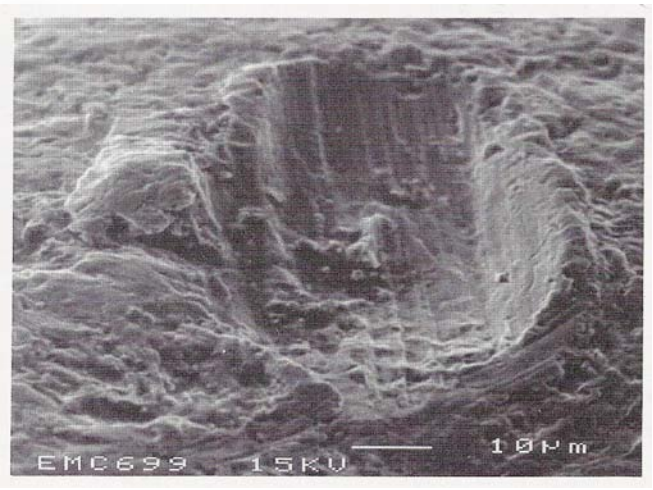

Figure 1.1 Cutting Mechanisms

a chip from target material resulting in the generation of new surface. The shape of impinging particle is main factor in cutting wear. Angular shaped impinging particles claims higher wear due to cutting. Because sharp edges of incident particles act as a cutting tool.

1.3.2) Ploughing Mechanism:

Ploughing wear takes place when a spherical particle stricks with larger negative rake angle on target material results in shearing and displacing the material in the form of raises lip at the side of creater and in front of the particle. The lip is formed in the direction of motion of erodent particle and above a certain critical velocity this lip removed from target material. This wear reported very less wear than other mechanism.

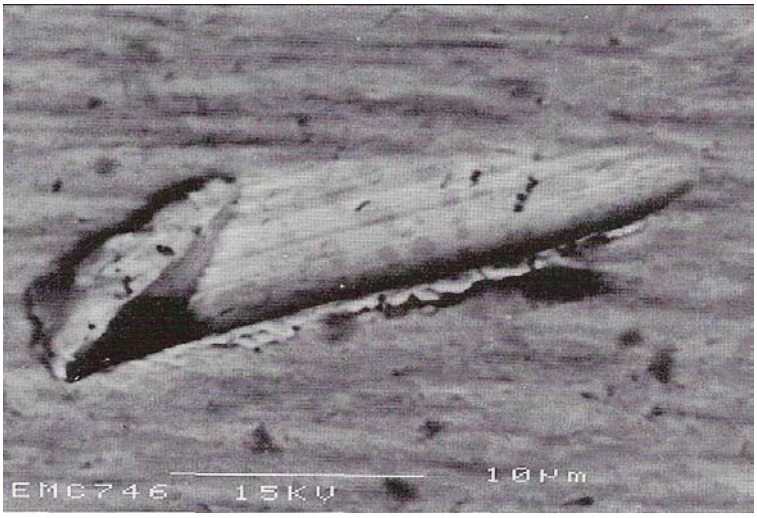

Figure 1.2 Ploughing Mechanism

1.3.3) Subsurface Deformation and Cracking:

When a spherical particle impacted on a target surface at high velocity plastic deformation of target material takes place at that point. This plastic deformation results in crater and cracks formation which propagate and results in wear by brittle fracture. An extruded shear lip is formed as a result of the particle collision. The shear lip broken off by fatigue caused by repeated impact of particles.

1.4) PARAMETERS AFFECTING EROSION WEAR:

The prominent parameters and their effect on erosion wear are as under:

1.4.1) Impact angle:

Impact angle is defined as the angle between the target surface and the direction striking velocity of the solid particle. The variation of erosion wear with the impact angle depends on the characteristics of the target surface material namely brittle or ductile type.

1.4.2) Velocity of solid particles:

Velocity of solid particle strongly affects the erosion wear. As particle velocity increases there is significant increase in erosion rate. The erosion rate is generally related to the particle velocity using power law relationship in which the power index for velocity varies in the range of 2-4.

1.4.3) Hardness:

Hardness is the characteristic of a solid material expressing its resistance to permanent deformation. Surface hardness as well as hardness of solid particles has profound effect on the erosion wear mechanism. Hardness ratio has been defined as the ratio of hardness of target material to the hardness of solid particles.

1.4.4) Particle size and shape:

Particle size and shape is also one of the prominent parameter, which affect erosion wear. Many investigators have considered solid particle size important to erosion. The erosion wear increases with increase in particle size according to power law relationship. The effect of particle shape on the erosion is not very well established due to difficulties in defining the different shape features. Generally roundness factor is taken into consideration. If roundness factor is one then the particles are perfectly spheres and a lower values show the particle angularity.

1.4.5) Solid concentration:

Concentration is amount of solid particles by weight or by volume in the fluid. As concentration of particle increases more particles strike the surface of impeller which increase the erosion rate, the concentration of slurries can vary from 2% to 50% depending upon the type of slurry. However, at very high concentrations particle interaction increases and this decreases the striking velocity of particle on the surface.

1.5) SLURRY:

Slurry can be a mixture of virtually any liquid combined with some solid particles. The combination of the type, size, shape and quantity of the particles together with the nature of the transporting liquid determines the exact characteristics and flow properties of the slurry. The

most commonly used fluid is water, however in some cases air is also used such as in pneumatic conveying. In homogeneous slurry solids are uniformly distributed throughout the liquid carrier. In heterogeneous slurry, solids are not uniformly mixed in the horizontal plane. Heavier particles tend to settle down and lighter particles tend to float.

1.6) COATING:

Coating is a covering that applied to the surface of an object, usually referred to as the substrate. Coatings are applied to improve surface properties of the substrate, such as appearance, adhesion, wetability, corrosion resistance, wear resistance, and scratch resistance. Coatings may be applied as liquids, gases or solids. Surface coatings include paints, drying oils and varnishes, synthetic clear coatings, and other products whose primary function is to protect the surface of an object from the environment.

1.7) METHODS OF COATING:

1.7.1) High velocity oxygen fuel (HVOF)

1.7.2) Plasma spraying

1.7.3) Powder coating

1.7.4) Electroplating

1.7.1) High Velocity Oxy-Fuel (HVOF):

During the 1980s, a class of thermal spray processes called high velocity oxy-fuel spraying was developed: A mixture of gaseous or liquid fuel and oxygen is fed into a combustion chamber, where they are ignited and combusted continuously. The resultant hot gas at apressure close to 1 MPa emanates through a converging–diverging nozzle and travels through a straight section. The fuels can be gases (hydrogen, methane, propane, propylene, acetylene, natural gas, etc.) or liquids (kerosene, etc.).

This process has been developed to produce extremely high spray velocity. The jet velocity at the exit of the barrel (>1000 m/s) exceeds the speed of sound. A powder feed stock is injected into the gas stream, which accelerates the powder up to 800 m/s. Powder may be fed axially into the

HVOF combustion chamber under high pressure or fed through the side of nozzle where the pressure is lower.

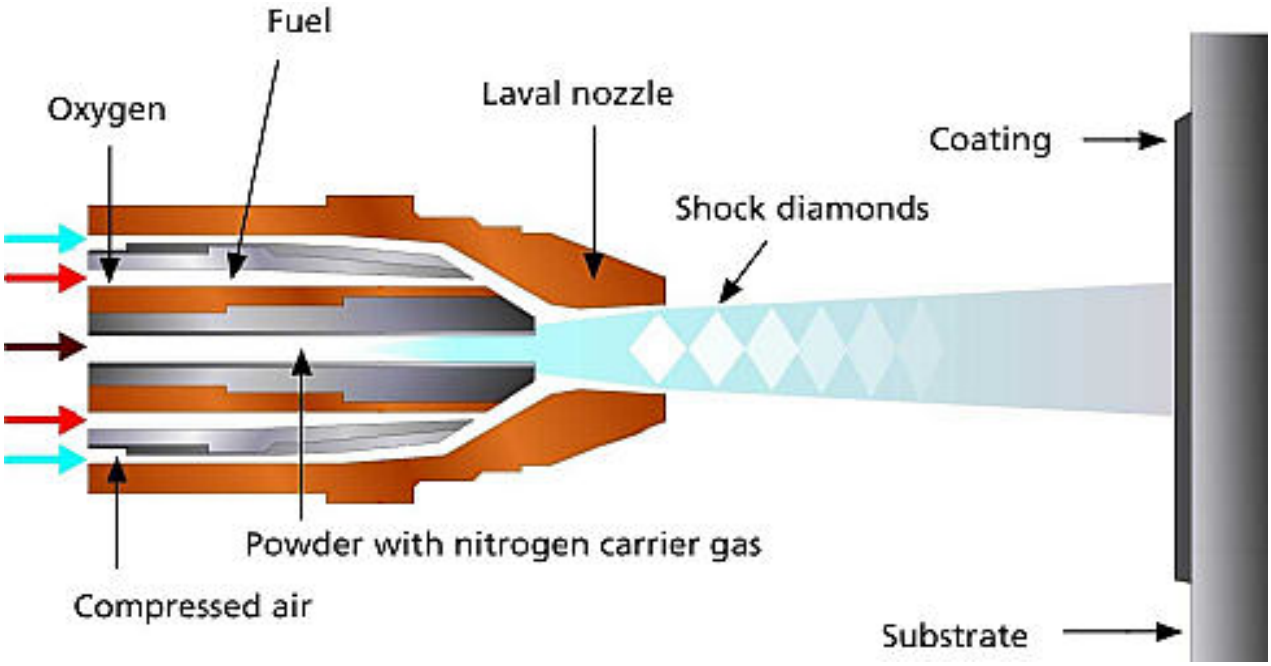

Figure 1.3 High Velocity Oxy-Fuel (HVOF)

The stream of hot gas and powder is directed towards the surface to be coated. The powder partially melts in the stream, and deposits upon the substrate. HVOF coatings are very dense, strong, high bond strength and show low residual tensile stress.

HVOF coatings may be as thick as 12 mm (1/2"). It is typically used to deposit wear and corrosion resistant coatings on materials, such as ceramic and metallic layers. Common powders include WC-Co, chromium carbide, MCrAlY, and alumina. The process has been most successful for depositing cermet materials (WC–Co, etc.) and other corrosion-resistant alloys like stainless steels, nickel-based alloys, aluminium, hydroxyapatite for medical implants, etc.

Advantageses:

(i) HVOF coatings are highest dense and strengthen found in most other thermal spray processes.

(ii) Lower flame temperature compared with plasma spraying

(iii) More favourable environment due to less oxidizing atmosphere

(iv) High compressive residual stress possible

(v) Strong adhesion to substrates

(vi) High cohesive strength, High density

(vii) Lower capital cost and ease of use compared to other processes

(viii) Reduced mixing with ambient air once jet and particle leave the gun

(ix) Thicker coatings than with plasma and arc spraying can be produced

(x) Process can be automated

(xi) Smooth as-sprayed surface finish and excellent machined surface finish.

(xii) Multiple choice of coating materials.

(xiii) Large volume reduction of hazardous waste and the associated disposal costs.

Limitations:

(i) Process, can only coat the external surface of a part, not the inner diameters.

(ii) There is a possibility of overheating the substrate material because the amount of heat generated in the HVOF stream is very high. Cooling of the substrate to the required level is very significant. Cooling is carried out either using liquid CO2 or air during spraying.

(iii) To date mechanical masking is effective but masking of the part is still a great problem. However design an effective mask for a complex component with areas is very difficult and indeed time consuming.

(iv) High capital cost.

1.7.2) Plasma spraying:

The Plasma Spray Process is basically the spraying of molten or heat softened material onto a surface to provide a coating. Material in the form of powder is injected into a very high temperature plasma flame, where it is rapidly heated and accelerated to a high velocity toward substrate. In the jet, the temperature is on the order of 10,000 K. The hot material impacts on the substrate surface and rapidly cools forming a coating. The plasma process uses very high electrical potential to disassociate ions from gases. As the gases reclaim their lost ions a tremendous amount of energy is released, mainly in the form of heat, which melts the powder.

The process also releases enough kinetic energy to accelerate the molten material toward the substrate.

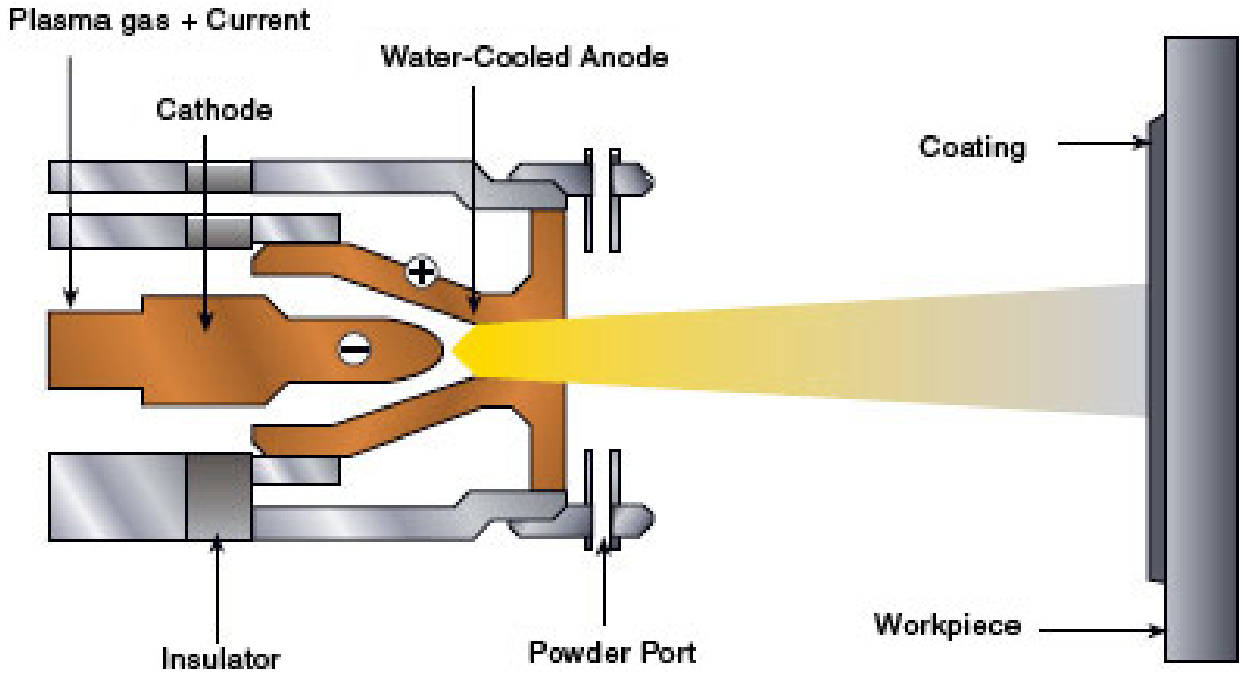

Figure 1.4 Plasma spraying

There are a large number of technological parameters that influence the interaction of the particles with the plasma jet and the substrate and therefore the deposit properties. These parameters include feedstock type, plasma gas composition and flow rate, energy input, torch offset distance, substrate cooling, etc. the substrate temperature can be kept low during processing avoiding damage, metallurgical changes and distortion to the substrate material.

Advantages:

(i) Almost any base material or substrate can be coated with the plasma spray process.

(ii) High bond strength is obtained.

(iii) The coating is stronger and denser.

(iv) Heat distortion problems are minimum.

Limitations:

(i) There is a high noise level ranging around 100 dB; this may damage the inner ear.

(ii) There is an intense ultraviolet and infrared radiation, which may cause sunburn, making it

essential to provide protection to eyes.

Applications:

(i) Plasma spraying is mainly used for producing wear resistant, temperature resistant, and heat insulating coatings,

(ii) Making rocket parts such as nozzles.

1.7.3) Powder coating:

Powder coating is by far the youngest of the surface finishing techniques in common use today. It was first used in Australia about 1967. Powder coating is a type of coating that is applied as a free-flowing, dry powder. The main difference between a conventional liquid paint and a powder coating is that the powder coating does not require a solvent to keep the binder and filler parts in a liquid suspension form. The coating is typically applied electrostatically and is then placed in an oven and the powder particles melt and coalesce to form a continuous film.The powder may be a thermoplastic or a thermoset polymer. It is usually used to create a hard finish that is tougher than conventional paint. Powder coating is mainly used for coating of metals, such as "whiteware", aluminium extrusions, and automobile and bicycle parts. Newer technologies allow

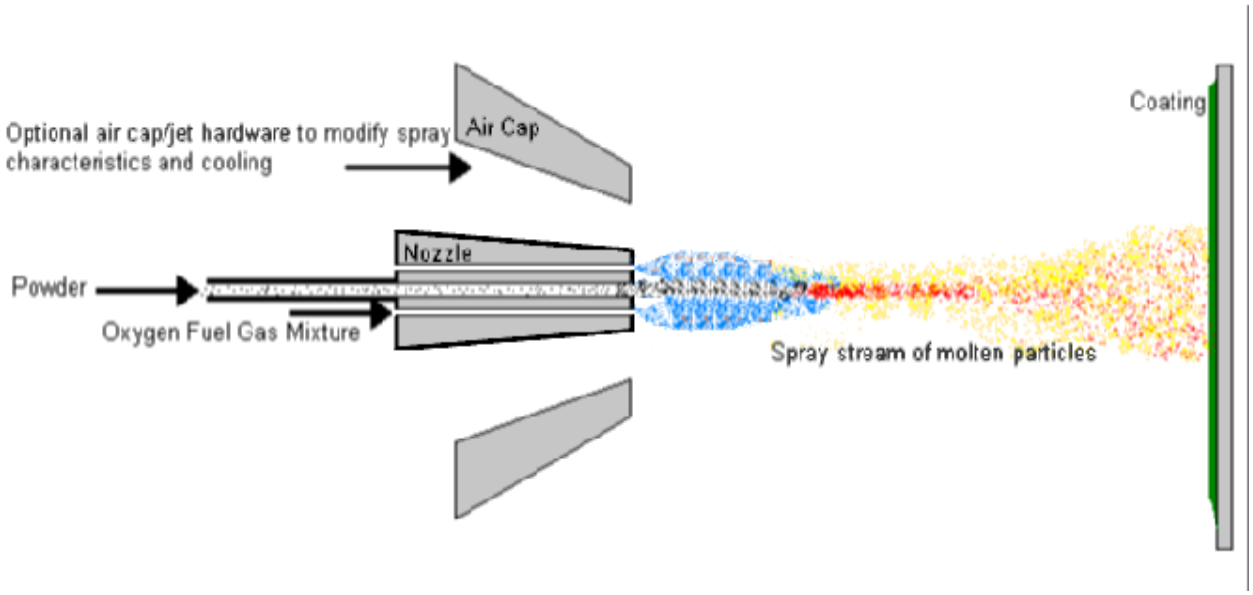

Figure 1.5 Powder Coating

other materials, such as MDF (medium-density fibreboard), to be powder coated using different methods.

Advantages:

(i) Powder coatings emit zero or near zero volatile organic compounds (VOC).
(ii) Exhaust air from the coating booth can be returned to the coating room, thus less oven air is exhausted to the outside.
(iii) Over-spray (up to 98%) can be retrieved and reused.
(iv) No drying or flash time required so that parts can be racked closer together
(v) Easily adapted to continuous, automatic processes.
(vi) Coating does not run, drip, or sag, thereby lowering rejection rates.
(vii) Minimum operator training and supervision.
(viii) Thick coatings are easily possible.
(ix) Simple clean-up and maintenance.

Limitations:

(i) Very thin coatings (less than 1.0 mil) are difficult because of pinholes.
(ii) Frequent color changes could entail extensive downtime.
(iii) Storage and handling of powder requires special climate controls.
(iv) Color matching and color uniformity is somewhat more difficult than with liquid coatings.
(v) Uniformity of coating thickness is sometimes difficult to maintain.
(vi) Cure temperatures required for some powders are too high for temperature sensitive parts.
(vii) Powder coating is difficult on sharp corners.
(viii) Conversion from liquid coating processes is expensive.
(ix) Inside corners have low film thickness owing to the Faraday cage effect.

1.7.4) Electroplating:

Electroplating is a plating process that uses electrical current to reduce cations of a desired material from a solution and coat a conductive object with a thin layer of the material, such as a metal. Electroplating is primarily used for depositing a layer of material for a desired property (e.g., abrasion and wear resistance, corrosion protection, lubricity, aesthetic qualities, etc.) to a

surface that otherwise lacks that property. Another application uses electroplating to build up thickness on undersized parts.

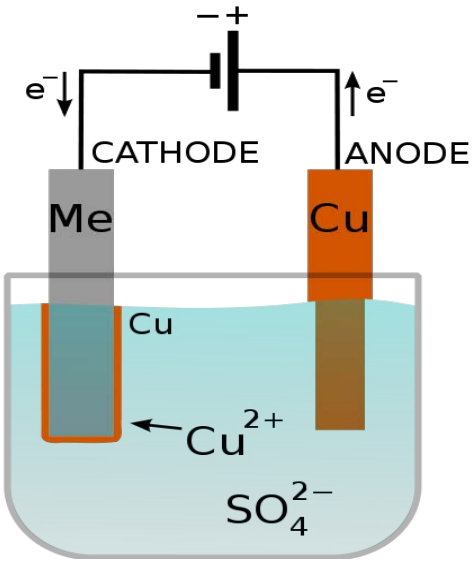

Figure 1.6 Electroplating Coating

The process used in electroplating is called electrodeposition. It is analogous to a galvanic cell acting in reverse. The part to be plated is the cathode of the circuit. In one technique, the anode is made of the metal to be platted on the part. Both components are immersed in a solution called an electrolyte containing one or more dissolved metal salts as well as other ions that permit the flow of electricity. A power supply supplies a direct current to the anode, oxidizing the metal atoms that comprise it and allowing them to dissolve in the solution. At the cathode, the dissolved metal ions in the electrolyte solution are reduced at the interface between the solution and the cathode, such that they "plate out" onto the cathode. The rate at which the anode is dissolved is equal to the rate at which the cathode is plated. The current flowing through the circuit and the ions in the electrolyte bath are continuously replenished by the anode.

Other electroplating processes may use a nonconsumable anode such as lead. In these techniques, ions of the metal to be plated must be periodically replenished in the bath as they are drawn out of the solution.

CHAPTER 2

LITERATURE REVIEW

Ahmed Elkholy et al. [1] studied the erosion wear of aluminium and cast iron having Brinell hardness 121 and 230 respectively by using the equation, $W = KV^n$. W is wear in term of mass loss of specimen per gram of sand. K is constant corresponding to other parameter like concentration of slurry, particle size and impact angle. The value of n determined by value of different velocities fitting in above equation. Then Belzona molecular ceramic steel (BMS) was test under identical condition as for Al and Cast Iron. The observation show that wear increase with increase in impact velocity. Impact Velocity affects more on BMS than Al and Cast Iron. He founded that the amount of wear varied with particle size with an exponent of 0.616. Study was conducted with 30º impact angle on cast iron. He assume that impact angle α is independent of velocity, an equation for wear of cast iron (hard and brittle) was established as

$$W = 1.061\times 10^{-8} [1+ \sin (\frac{\alpha - \alpha 1}{90 - \alpha 1} \times 180 - 90)]V^{2.3875} \quad \text{..... Eq. (2.1)}$$

α_1 is the angle at which wear develops and it is taken as zero for simplicity. Observations are taken at α= 60° and 90° with different velocities. The 90° impact angle showed higher wear for any arbitrary velocity value.

J. B. Zu et al.[2] designs a jet slurry erosion testrig. Using this testrig they tested rectangular specimens of aluminium, copper, mild steel (containing 0.15%C) and alumina. The size of specimens was 35mm×30mm with thickness 3-5mm. They observed the relationship between erosion rate and impact velocity for 600 - 1000µm silica sand slurry impinging onto aluminium. It was found that the material mass loss increase with increasing impact velocity according to power law, having an exponent δ(log E/δ(log v) = 2.7. They observed that the erosion of alumina (a brittle material), increases monotonically with impact angle, showing a maximum at near normal incidence. The erosion rate of the other metals in contrast increase with increasing impact angle only at small angles of incidence, with peak erosion at about 40º, and slowly decline at larger impact angles. All materials were tested at various parameters as slurry concentration (0-30%), impact velocity (0 to 8 ms^{-1}), impact angle (0º to 90º) and time. They observed that among all the four materials alumina show the lowest erosion rate, and aluminium the highest.

They found that the largest difference between the erosion resistance of alumina and other remaining materials occurs at a fairly small impact angle of near 30º-40º, where the metals all have their maximum erosion rates. The erosion resistance of alumina diminishes as the impact angle increases towards 90º. Among all four materials aluminium show maximum wear rate then copper followed by mild steel and alumina show lowest wear rate. They found that the mass loss increase with increase in erosion as straight line although some curvature toward a higher erosion time is after about 900min. the erosion rate rise slightly over the first 200 min then remain constant up to a time about 900min and a slow decline is then observed, this last decline due to degradation of the erodent particles. The initial rise in erosion rate (to 200 min) is due to the slow rise in temperature observed during the early running of the equipment. The maximum decline is reached after about 2300min.

Prasad BK et al[3] has studied the slurry wear behaviour of zinc-aluminium (Zn-59.8%, Al-37.5%, Cu-2.5%, Mg-0.2%) alloys with and without the addition of silicon content by the sample rotation method over a range of traversal speeds and distances. The alloys (Table 1) for conducting the experiments were prepared *via* the liquid metallurgy route in the form of 20 mm diameter, 150 mm long cylindrical castings. Cast iron moulds were used for solidifying the alloy melt in the required shape and size. The whole experiments were conducted in a test rig. An electric motor was used to rotate the samples in slurry over a range of traversal distances (15 to 500 km) and speeds (4.71 and 7.02 m/s). The slurry comprised 40% sand (212 to 300mm) particles suspended in an electrolyte (prepared by mixing 5 cc concentrated sulphuric acid and 4 g sodium chloride in 10 L of water). In his results he pointed out that wear rate of the samples increased with distance in the beginning, attained maximum, and then decreased thereafter at longer traversal distances and wear increases with increasing the traversal speed irrespective of the alloy composition. He also found out that addition of silicon improved the wear resistance (inverse of wear rate) of the alloy system.

Gandhi and Shesadri [4] has conducted the experiments on rectangular brass wear pieces (hardness=RC45, specific gravity=8.5) in a pot tester arrangement assuming the parallel flow wear i.e. the direction of impact velocity is parallel to the plane of wear surface. The range of the velocity was 3m/s to 9 m/s and three narrow size particulate slurries (890µm, 448.5µm and 223.5µm) were taken. The concentration of slurry was ranging from 20%-40%. In their results

they found that wear increases linearly with increase in velocity andthe slope of line increases by increasing any other parameter such as concentration and particle size. Based on the results, he established the relationship as follows:

$E_w = 2.57V^{2.56}C_w^{0.83}d^{0.85}$ ..... Eq.(2.2)

Where E_w= wear, V= velocity, C_w= Concentration, d= particle dia.

They concluded that parallel flow wear largely depends on the velocity as compared to solid concentration and particle size.

O.P. Modi et al[5] studied the erosion of high carbon steel in coal and bottom ash slurries with 30% concentration and 5 m/s sample rotational speed. It is observed that weight loss of H.C. steel specimen increase with increase in traversal distance 30% concentrated slurries of water +bottom ash and water+ coal. The test is conducted on both annealed and hardened steel for same experimental conditions. Initially the rate of increase in material loss was significantly high. Specimen attains a steady –state wear condition on further increase in traversal distance. At longer traversal distance difference between wear of annealed sample due to coal slurry & bottom ash slurry reduces. It is observed that weight loss of annealed steel was nearly 10 times more then hardened steel in both slurries with 30% concentration and 5 m/s sample rotational speed. It is observed that higher material loss of steel samples (Both annealed and hardened) in bottom ash slurry than in coal slurry has been caused by the presence of a large quantity of harder mineral constituents and less fracturing tendency of coal ash particles. The coal ash particles are softer and also get shatter during the process of erosion resulting in small pieces of reduced kinetic energy.

Craig I walker and Greg C. Bodkin[6] tested wear rate of side liner material (cast iron) on three assemblies (STD, HE and RE) at two tip speeds each with 1000µm sand particles size of 0.3 (by volume) concentration slurry. Speed did not show any marked effect on side liner wear rate, with the RE Impeller showing a slight increase and the HE a slight decrease with increasing speed. They also Observed that effect of sand particle size onside liner material (cast iron) wear was not significant for STD impeller. They also observed that wear rate for particle size 150µm, 500µm, 1000µm was nearly same. But for HE assembly it was the dominant variable. The wear rate is proportional to particle size.

O'Flynn et al[7] developed an analytical model for predicting the wear rate based on the toughness and strain energy of the target material. The model 24 is used to predict the erosion rate of heat-treated steels at different impact angles, which showed reasonable agreement with experimental measurements. They reported that the erosion resistance increases with increase in the value of the product of toughness and strain energy of the target material

C.I.Walker[8] compares the wear rate result of lab test and field test on side liner of STD and HE configurations of impellers. He found that the lab wear rate with cast iron material was greater than the wear rate for the field results with the white cast iron due to different hardness of parts. Both material show excellent similarities in wear rate trend with particle size. It is found from field result that rubber show lower wear rate than the metal for equivalent particle size < 700μm. This is because the rubber surface can absorb smaller particle impact energy without significant cutting tearing.

Gandhi et. al[9] observe that weight loss of a brass specimen increase with increase in volute angle and attained a maximum value at 178º angle with flow rate 18 lps. Slurry used is Zinc tailings material at 20% and 30% concentrations. For volute angle between 180º to 300º, the wear is smaller. He pointed out that the impact angle of solid particles decrease with increase in volute angle around 90º at tongue and nearly zero at nozzle. The wear along casing is the function of variation of impact angles of solid particles along the casing.

S.N. Singh and Gandhi[10] has conducted experiments in a pot tester for analysing the effect of orientation of plane surface relative to its motion in solid-liquid suspensions. They conducted experiments at various operating conditions by varying the impact angle, defined as the angle between the tangent to the plane surface and its velocity. Flat brass test pieces flush with a surface of hardened carbon steel plate (hardness= RC45) were taken. The orientation or impact angle was varied from 0° to 90° and concentration range was 20-40%. It has been found out that the erosion wear decreases with increase in orientation angle but this decrease was not consistent. It was seen that wear increases with the increase in orientation angle till 30° and then decreases with increase in orientation angle up to 90° for various range of velocities and particle sizes. Further it has been concluded that wear at 30° angle was 3-4.5 times higher than at 90° orientation angle and also wear increases with increase in velocity and particle size but decreases with increase in solid concentration under different impact angles.

Gandhi and Borse[11] had conducted experiments to determine the nominal size of multi-sized slurry representing the erosion wear and the effect of presence of fine particles (< 75µm) in the slurry. Wear specimens of grey cast iron were taken. The range of orientation angle was 0° to 90°. The slurry was prepared of water with sand collected from the banks of river Narmada. Overall specific gravity of sand was 2.68 and the final static settled concentration was observed as 53.7%. Mean particle size of slurry was taken as 505µm. The range for narrow size particulate slurry was 112.5µm to 855µm and multi sized slurry was prepared by mixing equal amount of different narrow sized slurries. Based on the results of their experiments they concluded that for narrow size slurry mean particle size can be taken as the effective particle size whereas for multi sized slurries, weighted mass particle size seems to be better. It has also been concluded that effect of finer particles in both narrow and multi sized slurries reduces the erosion wear.

Harry H. Tian, Graeme R. Addie[12] conducted experiment on erosion wear of soft ductile aluminium alloys and hard brittle high chromium white iron using coriolis wear test with slurries of different solids and concentration. The aluminium alloys tested were A380(a die cast grade) and 6061T-6511(an extruded grade). The high-Cr white irons were high- Cr iron (sand cast) and G75 high-Cr (centrifugal cast). The dimension of test specimen was 63.5mm×19.1mm×6.4mm. The test slurries were made of commercial grades of silica sand and clean water. Several particle sizes were used in the tests with mean diameter ranging from 22µm to 1428µm. The solids particles were of semi-rounded to semi-angular shapes. Coriolis wear tests were carried out at ambient temperature with a bowl speed of 975 rpm. They observed that higher the solid volume fraction the more frequently and strongly the solids contact and react with the target material, and more wear results. It was conclude that when slurry concentration increase from 1.52 vol.% solids to 12.12vol.%, the wear rate increased 187 – 204% on high-Cr (sand cast) material and by 298 – 468% on the aluminium alloy. It was observed that larger solid particles resulted in higher mass loss in all test materials. At slurry with 12.12 vol.% solids concentration and 15 gal/min flow rate, the wear rate increased about 20–28 times for the aluminium alloys and 42–45 times for the white iron materials as the mean diameter particle size increased from 22 µm to over 1400 µm. At 22µm (D50), the wear rate difference was only 4.3% between high-Cr (sand cast) and G75 white irons, and minus (–) 6.7% between aluminium alloys 380 and 6061T-6511. The wear rate difference grew to 10.3% between the white irons and to 29.9% between the aluminium alloys at the particle size of 1428 µm (D50). It was also found

that the wear rate ratio between the aluminium alloy 380 and white iron G75 was about 40 with very fine particles (22 μm D50). The wear ratio value peaked at around 150 with particle size between 100–200 μm and it decreased to about 27 with very coarse particles around 1400 μm. During the test it was found that a higher slurry flow rate generates more erosion wear but the percentage increase of wear rate was not as high as the percentage increase in flow rate. They observed that the much harder and stronger high-Cr white irons showed a tremendous advantage in wear resistance (up to 150 times) over the test aluminium alloys under the test conditions. Because Among the test materials, the extruded aluminium alloy containing limited alloy elements has the highest elongation/ductility.

K. Sugiyama et al.[13] were carried out slurry wear tests for base metal SCS6, HP/HVOF thermal-sprayed DTS-W110, arc-sprayed 56W2C/Ni/Cr and spray fused coating of self-fluxing alloy material 41WC/Ni/Cr/Co. The slurry jet test apparatus was used for the slurry wear test. The flow velocity was 10–40 m/s, and the impingement angle ranged from 90◦ to 15◦. The slurry concentration was 1 wt.%, consisting of 50 litres tap water and silica sand. The average diameter of sand particles was approximately 40μm. It was found that the volume loss rate of all test materials at 40 m/s is almost constant irrespective of impingement angle between 90◦ and 60◦, and decreases with a decreased angle. Coating hardness influences the slurry wear resistance of the thermal sprayed materials. The volume loss rate of SCS6 at an impingement angle of 90◦ increases with flow velocity, and is expressed by a power law. The volume loss rate in this study increases with flow velocity to the power of about 4. They also observed that slurry wear resistance of HP/HVOF-sprayed DTSW110, arc-sprayed 56W2C/Ni/Cr, and spray-fused 41WC/Ni/Cr/Co at 40 m/s is 86–143 times, 6–9 times, and 9 times, respectively, more than that of base metal SCS6.So slurry wear resistance depends on hardness of the thermal sprayed material. The resistance increases with hardness to about the third power.

C.N. Machio et al.[14] has studied the erosive wear of WC–12 wt.%Co and WC–17 wt.%Co as well as experimental WC–10 wt.%VC–12 wt.%Co and WC–10 wt.%VC–17 wt.%Co coatings deposited on stainless steel substrates using a high pressure high velocity oxy-fuel (HP/HVOF) thermal spraying system. The slurry consisted of the silica sand in water. An impeller circulated the slurry through a nozzle of diameter 12.5 mm. Tests were conducted at 45 and 90◦ incidence angles on specimens of size 50mm×50mm×6 mm. The results show that the WC–VC–Co

coatings exhibit higher erosion resistance then commercial WC- Co coatings. In slurry erosion, the best performance of the VC-containing coatings is as good as that of the commercial WC–Co coatings. They found that the erosion resistance of the WC–VC–Co coatings was similar to that of the commercial grades. This may be due to the (V,W)C grains being less resistant to impact fracture because of their higher hardness. They found that coatings with the higher cobalt content exhibited a higher wear rate because cobalt removal was the predominant wear mechanism.

S. Das et al.[15] studied the erosion-corrosion wear of aluminium alloy composites. The LM13 alloy and LM13-Sic composites were taken to study the effect of sand concentration on the wear behaviour in acidic and marine environment for a traversed distance of 763km and a rotational speed of 900rpm. They observed that the wear rate increase with increasing sand concentration irrespective of the material. This is because as the concentration of sand in the slurry increases the severity of erosion /abrasive attack increase because a greater number of particles are impinging on the surface. On the other hand, the slurry of corrosion attack may decrease because the effective volume of the corodent decreases. The alloy exhibited higher wear rate compared to the composite as sand concentration increased from 0% to 40%. It was concluded that all the material exhibited higher wear rate in the acidic media as compared to NaCl at 0% and 20%sand concentration. However at 30% and 40% sand concentrations the material posses lower wear rates in acidic media. The wear rate of all the materials decreased with distance traversed and approaches a constant value. However, the wear rate of LM13-10%Sic composite increased initially and then decrease to this value. In acidic slurry, the wear rate of the alloy approaches to a peak value and than decrease to a stable value. However, the wear rate of the composites decreased monotonically with distance traversed and attained a constant value at a long testing time. They note that the mass loss rates of all material increased when the speed was increased from 700 to 900 rpm. This is because the energy of impinging particle is directly proportional to the speed. When the speed was increased from 900 to 1100 rpm, the mass loss rate decreased irrespective of the material and solution type. This is because at higher speed the sand particles simply slide over the surface instead of making any sensible impact. Also at high speeds, the chances of inter collision among the erodent particles are more. Since corrosive attack was more severe in NaCl medium then in acidic medium when slurry consisted of 30wt% of sand. So these materials experienced greater wear rates in NaCl medium than in acidic medium at all speeds.

G.R desale et al[16] conducted an experiment to show the variation of erosion rate with orientation angle for solid liquid mixture of three natural erodent (quarts ,alumina ,and silicon carbide) for ductile target material AA 6063 and A1513042 steels the test performed in a pot tester rotating specimen at 3 m/s in 10wt% concentrated slurry having particle size 550µm. As the orientation angle increase then erosion rate I_{st} increase up to a maximum and then decreases to a steady state till 90º. Both the target material show maximum wear at shallow angles with all three erodents. The max wear angle observed as 15º and 22.5º for AA6063 and AISI 304L steel respectively. Then it concluded that angle for maximum wear is a function of target material properties and do not depends on erodent properties.

M.C. Lin et al.[17] conduct experiment to study high-speed slurry erosion characteristics on the test specimens of NiCrBSi coating prepared by using the high velocity oxy-fuel spraying technique with a post-thermal treatment. The composition of powder used for spraying is Ni–17Cr–3B–4Si–4Fe–1C (wt.%). The sprayed coating had a 1.5 mm thickness and exhibited a melting temperature of 1050 °C. The substrate used was AISI 1045 carbon steel. Sand water mixture with particle size of 263-363µm is used as impingement medium. SUS304 stainless steel was selected as the comparison material. Experimental results show that the NiCrBSi sprayed coating exhibits a much better slurry erosion resistance than the SUS304 stainless steel because of he post-thermal-treated NiCrBSi coatings have an extra high hardness and small quantity of porosity. A preliminary test has revealed that the NiCrBSi spray coating can increase significantly the using-life, 3–4 times, of needles and nozzles in hydraulic machinery. The erosion rate for the NiCrBSi sprayed coating slightly increases with the impinged angle. However, a maximum erosion rate appears at an impinged angle of around 30° for SUS304 stainless steel. Both NiCrBSi sprayed coating and SUS304 stainless steel exhibit impinged surfaces with lots of furrows at an impinged angle of 30°. At a high impinged angle of 90°, the SUS304 stainless steel exhibits an impinged surface with lots of overlapping and irregular concavities, while, these features are less obvious for NiCrBSi sprayed coating. The hardness of SUS304 stainless steel increases significantly with increasing impinged angle during the high-speed slurry erosion. But, there is no obvious work hardening for the NiCrBSi sprayed coating due to its extra-high hardness and less plastic deformation, even at a high impinged angle of 90°. The surface morphologies exhibit lots of long furrows and ridges at a low impinged angle of 30°, regardless of the SUS304 stainless steel or NiCrBSi sprayed coating. At a high impinged angle

of 90°, the SUS304 stainless steel exhibits an impinged surface with lots of overlapping and irregular concavities due to the deformation of microforging and extrusion. However, these features are less obvious for NiCrBSi sprayed coating, due to its extra-high hardness and the micro-porosities existing within the sprayed coating.

T. Manisekaran et al.[18] had studied the effect of particle size and impingement on surface modified 13Cr-4Ni stainless steels (as they are generally used for hydro turbines and water pumps). Samples of dimension of 50×50 mm^2 were machined from 6 mm thick cast 13Cr-4Ni steel plates and the surface modifications were done by two methods namely laser hardening and pulsed-plasma nitriding. Tests were carried out in a test rig to study the erosion performance of modified layers with two different erodent particle size ranges (less than 150 and 150-300 lm) in a silica sand slurry for 2 h at 90°. After surface modification they observed that pulsed plasma hardened steels showed more hardness than laser hardened steels but based on their experiments they found interesting results that laser hardening of 13Cr-4Ni steels exhibited better erosion resistance at all angles of impingement than pulse plasma nitriding. It had also been concluded that the amount of erosion with erodent size range 150-300μm was two times more than the amount of erosion with erodent size range less than 150 μm and SEM examination clearly revealed that plastic-deformation mode was primarily responsible for material removal in laser-hardened steels.

M.N. Noui-Mehidi et al [19] has experimented the effect of paint layers on stainless steel specimen in a slurry-mixing tank in which 10 painted samples mounted on a shaft were rotated at constant speed for a certain interval of time. The slurry was a mixture of tap water and alumina particles with a concentration of 15% (v/v). Different type of paints such as Gloss Enamel paint, Epoxy Enamel, Standocryl 527 two-pack paint etc were applied on steel specimen by spray guns operated with compressed air. The effect of impact angle on the particular type of paint was investigated by orientating the samples consecutively at angles from 0◦ to 90◦ with an increment of 10◦. They found that in the slurry medium, most soft paints, such as “Enamel” type have similar erosion maps to ductile materials with a maximum wear rate at around 30◦. Metallic paints and styrene type paints have shown a slightly higher angle of 40◦ for maximum erosion.

Y.A. Khalid et al.[20] has designed and fabricated wear testing rig to analyse and to select parameter that can be used to determine the wear rates of slurry pump impeller. In his

experiments he used an open type impeller made of cast iron with 165mm diameter and five numbers of blades. The slurry used consists of solid- liquid mixture of sand and crushed stones with water. He found out that the weight loss of the impeller is due to the material removal from the impeller as a result of erosion wear. The material is removed from several locations such as circumference, thickness of the blade, height of the blade and depth of the impeller shroud (base). Among these parameters, height loss of the blade represents the highest percentage of 60.86 percent followed by thickness loss of the blade of 35.09 percent, while the diameter loss of the impeller has the lowest loss that is 2.30 percent. All these percentage values are related to the original values. Further it has also been concluded that the region near the center of impeller encounter less wear compared to the region at the rim of the impeller. The surface topography at the rim of the impeller showed that the materials are removed in the tangential direction to the impeller.

A.A.C. Recco et al.[21] was studied the combination of different surface treatments for improving the erosion resistance of an AISI 304 stainless steel. Six kinds of sample conditions were tested in a slurry composed of distilled water and SiC particles; High temperature gas nitriding (HTGN), low temperature plasma nitriding (expanded austenite), high temperature gas nitriding followed by a PVD-TiN coating, low temperature plasma nitriding followed by a PVD-TiN coating as well as PVD-TiN coated and uncoated samples in the solubilized condition. The erosion tests were performed during 6 h in a jet-like device with a normal angle of incidence and an impact velocity of 8.0 m/s. The results show that the wear rate of the austenitic stainless steel reduced by 1.5 times in high temperature gas nitriding, reduced by 2 times in low temperature pulsed plasma nitriding. Also PVD-TiN coatings deposited over different surface treatments of the austenitic stainless steel reduced the wear rate by 20 times. They conclude that the mechanical properties of the substrate did not affect the erosion rate of the TiN coated specimens. When the TiN coating is removed, the effect of the substrate hardness differences is observed and intense cutting of the samples is observed.

Desale et al.[22] carried out erosion wear tests using seven different ductile type materials namely aluminium alloy(AA6063), copper, brass, mild steel, AISI 304L stainless steel, AISI 316L stainless steel and turbine blade steel using three different erodents namely quartz alumina and silicon carbide which have been mixed with water to prepare three different solid liquid

mixtures. Experiments were conducted using a slurry pot tester by orienting the wear specimens normal to their rotational direction. The mean size of erodent was taken as 550μm. Different combinations of erodents and target materials were taken. It was observed that wear at normal impact condition is a strong function of hardness ratio which is defined as the ratio of hardness of erodent and target materials. Experiments were also conducted for different solid concentrations, particle sizes and velocities. Based on the experimental data Gandhi developed a correlation to estimate the erosion wear rate for normal impact condition. $E_{d90}=6.62\times10^{-14}\times K_{(Hp/Ht)}V^{2.02}d^{1.62}C_w^{-0.285}$.....Eq.(2.3)

where V is the velocity of impacting particle in m/s; d the particle size in μm; C_w the solid particles concentration in wt%; $K(H_p/H_t)$ is a constant, which is a function of the hardness ratio and is express as under,

$K_{(Hp/Ht)} = 0.42$, for $H_p/H_t \leq 6$

$K_{(Hp/Ht)} = 1.0$, for $6 \leq H_p/H_t \leq 12.3$

And

$K_{(Hp/Ht)} = 1.83$, for $12.3 \leq H_p/H_t$

The above correlation (Eq. (2.3) is used to estimate the normal impact wear of different target materials using the three erodents and the predicted values are compared with the measured values to determine the accuracy of the fit. Further it has been concluded from SEM micrographs and surface roughness measurements that the penetration by solid particles at the target material surface is a function of hardness ratio. Also erosion wear due to normal impact has strong dependence on velocity and particle size but relatively weak dependence on solid concentration.

N. M. Dube et al.[23] studied the effect of slurry turbulence on wear with a counter rotating double disc erosion tester developed by DUCOM. In this experiment they use two discs (dia 160mm and thickness 2mm) of aluminium and stainless steel (ss-304) placed co-axially and rotates at equal rate in opposite direction with the help of two induction motors. The discs are fixed at the end of each of motor shaft. The distance between discs can be varied to generate the turbulence in slurry chamber. Silica and alumina are used for making slurry. The concentration of both the slurries varies from 14% to 55% in step of 7% and keeping angular 1500 rpm and

time constant (1h). They found that wear increase with increase in particle concentration (wt. fraction) the result shows that wear increases linearly with particle concentration in all cases except wear on stainless steel by alumina. Alumina slurry shows a slight decrease in wear of stainless steel between 0.25 to 0.35 concentrations. During test they founded that the wear on stainless steel disc (ss-304) is less compared to aluminium in all the three parameters; time (0.5-3h), angular speed (1000-3000rpm) and concentration (14- 55%). This is because of high yield strength of the stainless steel than aluminium. The concentration of slurries is taken as 40% and angular speed varies from 1000-3000rpm.Then it was observed that increased in the angular rate increases the turbulence and hence increase in the weight loss of discs. The effect of wear is higher in alumina slurry over the range of angular speed. The alumina slurry causes the higher volume loss then silica slurry identical testes conditions because alumina is harder than silica particles.

J.F. Santa et al. [24] studied the slurry and cavitation erosion resistance of six thermal spray coatings in laboratory and compared to that of an uncoated martensitic stainless steel. Nickel, chromium oxide and tungsten carbide coatings were applied by oxy fuel powder (OFP) process and chromium and tungsten carbide coatings were obtained by high velocity oxy fuel (HVOF) process. The microstructure of the coatings was analyzed by light optical microscopy (LOM) and scanning electron microscopy (SEM), as well as by X-ray diffraction (XRD). The slurry erosion tests were carried out in a modified centrifugal pump in which the samples were conveniently placed to guarantee grazing incidence conditions, as well as in a high velocity jet erosion testing machine. The results showed that the slurry erosion resistance of the steel can be improved up to 16 times by the application of the thermally sprayed coatings. On the other hand, none of the coated specimens showed better cavitation resistance than the uncoated steel in the experiments. The main mass removal mechanisms observed in all the coatings submitted to slurry erosion were micro-cutting and microploughing as well as detachment of hard particles.

Gandhi and Disale[25] had conducted experiments in a pot tester to investigate the effect of particle size on erosion wear of aluminium alloy 6063 (AA 6063). Narrow sized particulate slurry of Indian standard sand (quartz) with mean size varying in the range of 37.5-655µm were used at 3m/s velocity for 20% wt. concentration of solids at 30°-90° orientation angles. Further it was concluded that there exists minimum kinetic energy of the particles, which changes

mechanism of material removal from erosion to three body abrasion. Due to three body abrasion, the wear due to smaller sized particles is little higher compared to that of bigger size particles.

Zhou Guanghong, Ding Hongyan[26] has studied the corrosion–erosion wear behaviours of austenitic stainless steels, 316L and 13Cr24Mn0.44N in water–sand slurry and saline–sand slurry, respectively. The corrosion–erosion wear mass-loss was measured to evaluate the influence of medium and materials. The specimen material was austinised and oil quenched and finally annealed to relieve internal stresses. The wear experiments were performed in a modified solid particle slurry corrosion–erosion wear apparatus.

They calculated the wear in terms of relative wear resistance (ε) and synergism ratio (η) where: -

$\varepsilon = W_s/W_{c,}$ ..... Eq.(2.4)

W_s is the mass-loss of 316L; W_c is that of 13Cr24Mn0.44N under the corresponding condition.

And $\eta = (M_{corr}-M_{water})/M_{corr,}\ M_{corr}$ ..... Eq.(2.5)

η is the entire mass-loss after corrosion–erosion in the saline–sand slurry; M_{water} stands for the mass-loss after abraded in the water–sand slurry. Based on the results they concluded that the mass-loss ratio of 316L is always larger than that of 13Cr24Mn0.44N whether in saline–sand slurry or in water–sand slurry. The relative wear resistance increases with the increasing of the impingement velocity and arrives at maximum of 1.6. Both the stainless steels present a positive synergism between wear and corrosion. Further, the dominant wear mechanism of 13Cr24Mn0.44N is abrasive wear in the water–sand slurry, whereas it becomes abrasive wear associated with little corrosive pitting in the saline–sand slurry. As for 316L, the dominant wear mechanism is also abrasive wear in the water–sand slurry, whereas it becomes abrasive wear associated with corrosive delamination fatigue in the saline–sand slurry.

M. M. Stack et al[27] studied the combined effects of slurry particle concentration and velocity on the erosion–corrosion of a WC/Co–Cr coating in a synthetic seawater solution containing sand particles and compared to the performance of a mild steel exposed to similar conditions. They used specimens of size 20mm×10mm×3mm having thickness of the coating varied in the range of 8–13 μm and 0.196 cm^2 area exposed to impingement slurry jet. They set the test samples at a fixed impact angle of 90° to the impinging jet and a test conducted for 30 min. The

seawater slurry composed of silica sand with particle size in the range 50–250 µm and concentration varied at three values 4%, 6% and 8% (by mass %), and at two impact velocities namely 2 and 4 ms^{-1}.

Y. Iwai et al[28] has conducted a Micro-Slurry-jet Erosion (MSE) test to swiftly evaluate the wear properties of thin single layered and multilayered coatings deposited on cemented carbide. Slurry containing 1.2µm alumina particles (hardness from 1800 to 2000 HV) was impacted at high velocity (around 100 m/s) perpendicular to CVD TiC/TiN (TiN on top of TiC) and TiC coatings. The test piece was a square of 12.8mm with 5mm in height. In case of CVD TiC/TiN coating they observed that wear depth of the TiN layer increased linearly until the TiC layer was reached, where after it first increased steady at a lowslope but tended to increase during the passage of the coating/substrate interface. They conclude that wear resistance of the TiC layer was about two times higher than that of the TiN layer. The experiment shows that wear rates were constant within the TiN and TiC layers, but showed significant changes near the interfaces, especially that between the coating layer and the substrate. They observed that the wear rate of the TiC layer for the TiC/TiN coating almost coincides with that of the single layered TiC, and was about half of that of the TiN layer. They proved that TiC layer have about two times higher wear resistance than the TiN layer.

R.C. Shivramamurthy et al[29] has conducted experiments to study the slurry erosive wear mechanisms of Co-based Stellite and Ni-based Colmonoy coatings on 13Cr-4Ni steels applied by Laser surface alloying (LSA) method. They perform experiment for a constant slurry velocity of 12 m/s, for a fixed slurry concentration of 10 kg/m3 sharp-edged SiO2 particles with average sizes of 375 and 100 µm and at impingement angles of 30º, 45º, 60º, and 90º. They pointed that when coatings impacted with slurry particles of an average size of 375 µm then stellite coating showed ductile behaviour whereas brittle in case of colmonoy. Only a brittle behaviour was observed in both coating when impacted with slurry particles of an average size of 100 µm. They found that the erosion rate decreases in the coatings and the erosion rate in case of Ni-based steel is less as compared to Co- based coated steels.

M. Hadad et al[30] studied and compared the slurry and dry erosion wear behaviour of Cermet based WC–Co–Cr thermally sprayed coatings deposited by high velocity oxy-fuel (HVOF) spraying on steel substrate. They deposited different bond layers on specimens of size 40 mm×

40 mm, the first cermet coating, and then a cermet top coating was sprayed to form the sandwich structure. Ni–Cr 80–20 and Co–Cr were deposited by HVOF spraying on the first cermet coating then nickel was electrochemically plated on the cermet coating. Both slurry and dry erosion tests performed by jet impingement erosion tester at two different incident angles of 90 and 30◦ and Al_2O_3 as erodent particles. It was pointed that the combination Co–Cr as interlayer showed the lowest wear resistance, whereas, the combination Ni–Cr 80–20 interlayer showed the highest wear resistance under impact angle of 90 . They observed that the wear rate in slurry erosion under 30◦ showed higher than that under 90◦ and also, wear erosion rate in slurry erosion is about 10 times smaller than that in dry erosion under both angles.

S.C. Mishra et al.[31] studied all the parameters affecting the erosion wear using jet erosion tester on fly ash-quartz coating. By varying different parameters they evaluated that impact angle is the most significant factor influencing the erosion wear of fly ash-quartz coating. They also evaluated that maximum erosion takes place at impact angle of 90°.

BS Mann et al.[32] compared erosion behavior of WC10Co4Cr, Armcore 'M', Stellite 6 and 12 HVOF coatings, TiAlN PVD coatings. Impact angle of 60° and velocity of 20m/s was kept constant for all experiments. Mineral sand was used as solid particles of slurry. They concluded that WC10Co4Cr HVOF coatings show best performance against slurry erosion. They also evaluated the corrosion performance and found that WC10Co4Cr HVOF coating corroded significantly. WC10Co4Cr HVOF coatings have very good erosion resistance but not corrosion resistance.

Neville et al.[33] studied the erosion-corrosion behavior of WC-Metal Matrix Composites(EFM, EFW, EGC, EGG). The materials were eroded by two sizes of silica sand with stream velocities of 10 and 17 m/s at 65 ◦C. Test was conducted by varying the concentration. They evaluated that WC grain size fractions has very little effect on wear. They also concluded that the erosion–corrosion rate is strongly dependent upon erodent size, impinging velocity and solid loading.

Factor et al.[34] evaluated the erosion wear using solid particles in He gas of Wc-17Co and $Cr_3C_2 + 25NiCr$ coatings on steel alloy using Sic as erodent. They evaluated that coating helps in reducing the erosion wear. At an angle of 90° Wc-17Co shows the better result but a low impact angles $Cr_3C_2 + 25NiCr$ was better.

CHAPTER 3

STUDY OF PROPERTIES OF FLY ASH

Fly ash is one of the residues generated in combustion, and comprises the fine particles that rise with the flue gases. Ash, which does not rise, is termed bottom ash. In an industrial context, fly ash usually refers to ash produced during combustion of coal. Fly ash is generally captured from the chimneys of coal-fired power plants, and together with bottom ash removed from the bottom of the furnace, jointly known as coal ash. Fly ash includes substantial amounts of silicon dioxide (SiO_2) (both amorphous and crystalline) and calcium oxide (CaO). The fly ash may contain higher levels of contaminants than the bottom ash.

Figure 3.1 Fly Ash Image

Toxic constituents depend upon the specific coal bed makeup, but may include one or more of the following elements or substances in quantities from trace amounts to several percent: arsenic, beryllium, boron, cadmium, chromium, chromium VI, cobalt, lead, manganese, mercury, molybdenum, selenium, strontium, thallium, and vanadium, along with dioxins and PAH compounds. In the past, fly ash was generally released into the atmosphere, but pollution control equipment mandated in recent decades now require that it be captured prior to release. Fly ash is generally stored at coal power plants or placed in landfills. The reuse of fly ash as an engineering material primarily stems from its pozzolanic nature, spherical shape, and relative uniformity. The chemical composition of Indian fly ash is showing in table 3.1.

Table 3.1 Chemical Composition Fly Ash.

	COMPOSITION		
Component	**Bituminous**	**Sub-bituminous**	**Lignite**
SiO_2	20-60	401-60	15-45
Al_2O_3	5-35	20-30	10-25
Fe_2O_3	10-40	4-10	4-15
CaO	1-12	5-30	15-40
MgO	0-5	1-6	3-10
SO_3	0-4	0-2	0-10
Na_2O	0-4	0-2	0-2
K_2O	0-3	0-4	0-4
LOI	0-16	0-3	0-5

Fly ash reuse in Portland cement, Embankments and structural fill, waste stabilization and solidification, raw feed for cement clinkers, mine reclamation, Stabilization of soft soils, road sub base and other applications include cellular concrete, geopolymers, roofing tiles, paints, metal castings, and filler in wood and plastic products.

To study the different properties of fly ash and its slurry, the ash collected from Guru Gobind Singh thermal power plant Ropar (Punjab). The properties of fly ash is studied and discussed below.

3.1) PARTICLE SIZE DISTRIBUTION (PSD):

The percentages of each fraction into which a granular or powder sample is classified with respect to particle size, by number or weight. Sieve analysis and hydrometer analysis are the two methods used for determination of the distribution of particle size. Hydrometer analysis is used for finer particles, which are below 75 microns whereas sieve analysis is performed to determine the particle size of coarse particles i.e. particle size greater than 75 microns. To determine the PSD of fly ash, a known weight of fly ash is taken and washed over a B.S. 200 mesh (75 μm). The ash retained over the sieve as well as under (which is of fine particles) is dried in an oven.

The dried coarser ash is sieved through a set of standard sieves (in figure 3.3). The figure below showing the SEM image of fly ash particles.

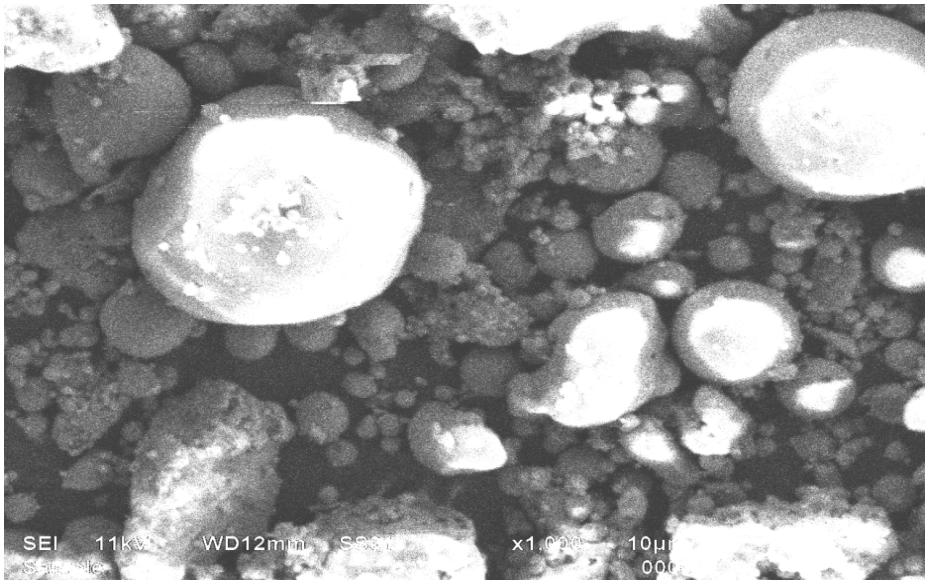

Figure 3.2 SEM Image of Fly Ash

The ash retained on each sieve is collected and the percentage retained on each sieve calculated using the standard procedure. Then standard hydrometer analysis performed to determine the particle size distribution of fine particle (size less than 75 microns) collected.

Figure 3.3 (a) Standard Sieves

Figure 3.3 (b) Sieve Shaker

The experimental result of particle size distribution of fly ash is showing in table 1.1 in Annexure I. The graph for PSD plotted between particle size and percentage finer (by weight) as shown in figure below.

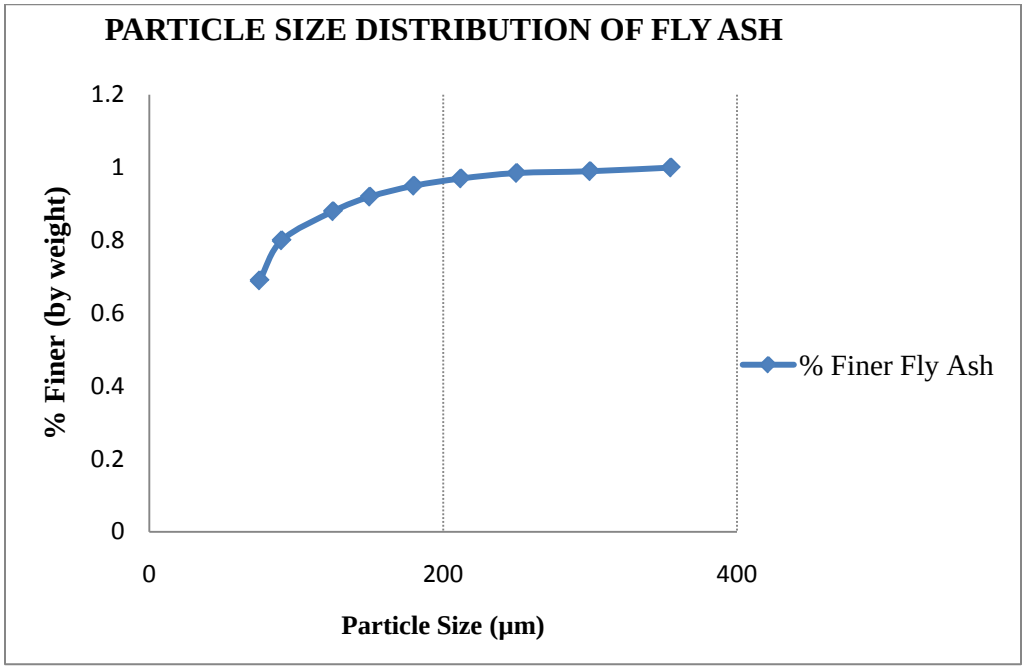

Figure 3.4 Particle Size Distribution of Fly Ash

3.2) STATIC SETTLED CONCENTRATION:

The static settled concentration decides the highest limit of solid concentration, which can be achieved by gravitational settling. The static settled concentration depends on parameters like density and viscosity of carrier fluid and specific gravity, shape and size distribution of solids. In the present study, the static settled concentration of fly ash slurry of overall 20% concentration (by weight) has been determined. The experiment performed according to procedure discussed below.

The fly ash of known amount according to concentration of 20% by weight was taken. First, fill the jar with the known quantity of water and then put the required amount of fly ash in it. Then leave the jar for 2 hours. After 2 hours close the mouth of the jar by hand or some source and mix vigorously it by keeping the jar upright. The level of the ash in the jar noted w.r.t. to time in each 10 sec. The time interval increase for further readings, which is shown in Table 1.2,

Annexure II. The readings noted until we get the static steady state. Then graph plotted between the static settled concentration as ordinate and time as abscissas, shown in figure 3.5.

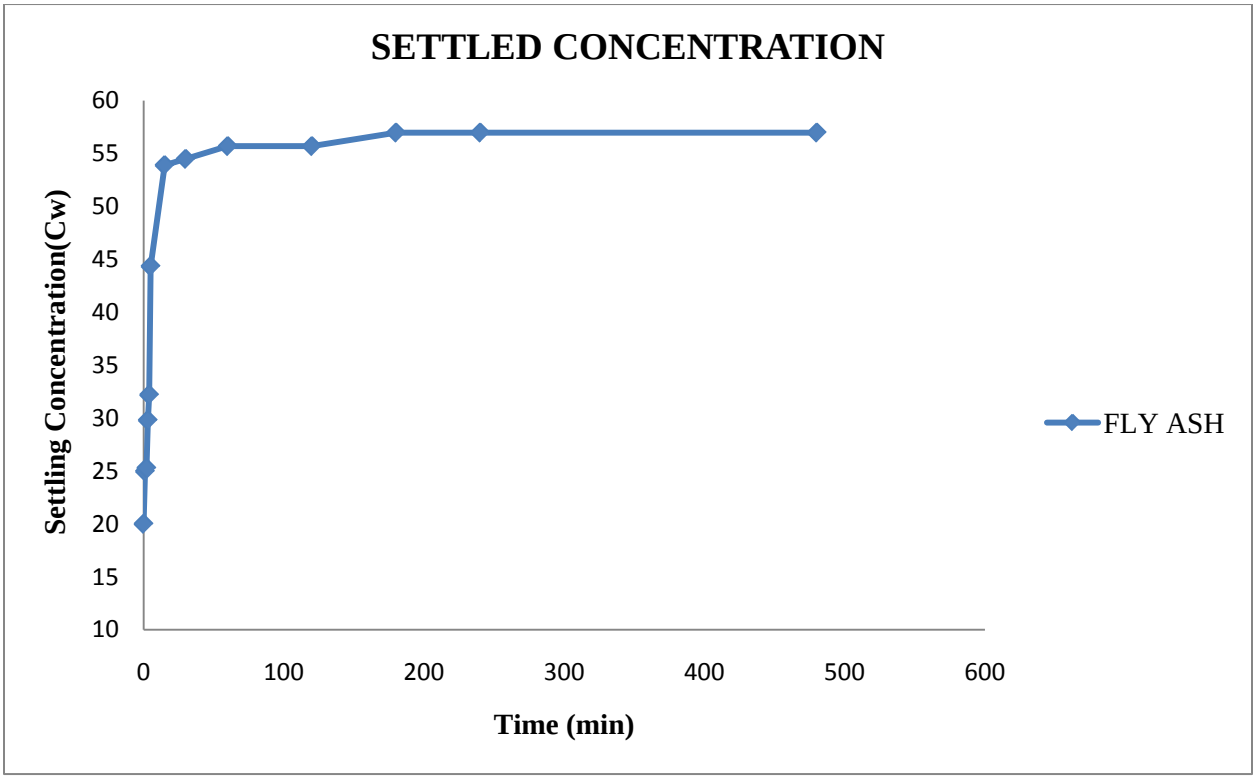

Figure 3.5 Static Settled Concentration of Fly Ash

3.3) SPECIFIC GRAVITY OF FLY ASH:

The pyknometer test is employed to determine the specific gravity of fly ash. Firstly the pyknometer (capacity 50 ml) is cleaned and kept in an oven to remove the moisture content from it. Pyknometer is taken from oven after 2 hours and cooled down and weighted (W_b). After that about 30 gms of over dried fly ash is put in pyknometer and weighted (W_{bs}) again. Then a small amount of water is poured in it and mixture shaken simultaneously. It should be ensure that no air entrapped in pyknometer during pouring. The opening of the pyknometer is closed with thumb and mixed vigorously for 5 minutes and then left the mixture for 2 hours to escape the air bubbles formed during the mixing. After 2 hours, completely fill the pyknometer with water and cork it. Then weight pyknometer (W_{bsw}) after cleaning its outer surface. Now empty the pyknometer, dry it, and fill it with distilled water and weight it (W_{bw}). Then specific gravity of fly ash can be calculated by the following formula:

$$\text{Specific gravity} = \frac{(Wbs - Wb)}{\{(Wbw - Wbsw) + (Wbs - Wb)\}}$$

Where,

W_b= Weight of Beaker, W_{bs}= Weight of beaker and solid

W_{bw}= Weight of beaker and water, W_{bsw}= Weight of beaker solid and water.

The specific gravity of fly ash is comes out 1.923 after conducting all above observations.

3.4) RHEOLOGY:

Rheology is the study of the flow behaviour and deformation of a fluid or a semisolid when subjected to forces. Viscosity plays important role in the estimation of energy required for transporting slurry through pipelines. The solid particles, which are present in a carrier fluid, alter its viscosity. A Non-Newtonian behaviour shown by solid-liquid mixture as solid added in carrier fluid beyond a certain limit. To establish the rheology of flyash-water mixture, the variation of shear stress with shear rate has been obtained over a range of concentrations varying from 10 to 40% (by weight).

3.4.1) Rheological Measurements:

The shear stress-shear rate relationship for fly ash slurry can be determined by using bob and cup geometry (in figure 3.6 b) of rheomete (make Anton paar). The geometry consists of a fixed cylinder (bob) and a rotating cylinder (cup). The slurry placed between the annular space between the two cylinders and a torque applied on the rotating cylinder (cup). The viscosity of slurry obtained by the graph plotted between shear stress and strain rate. Figure 3.6 (a) showing the rheometer used for present investigation**.** Newtonian or Non-Newtonian behaviour of fly ash slurry has been identifies by measuring the variation of shear stress with shear rate over a range of concentrations. The shear rate given as an input in the rheometer and corresponding shear stress obtained as output. The fluid will show the Newtonian behaviour when the graph shows linear relationship between shear stress and shear rate and if it deviates from linear curve, fluid will show the Non-Newtonian behaviour.

Figure 3.6 (a) Rheometer (Anton Paar) **Figure 3.6 (b) Cylindrical cup and rotating Bob**

Table in 1.3 Annexure II shows the experimental results of shear stress and shear rate and table 1.4 in Annexure III showing the relative viscosity over a range of concentrations. The graphs of shear stress and shear rate and relative viscosity showing below in figure 3.7 and 3.8 respectively**.**

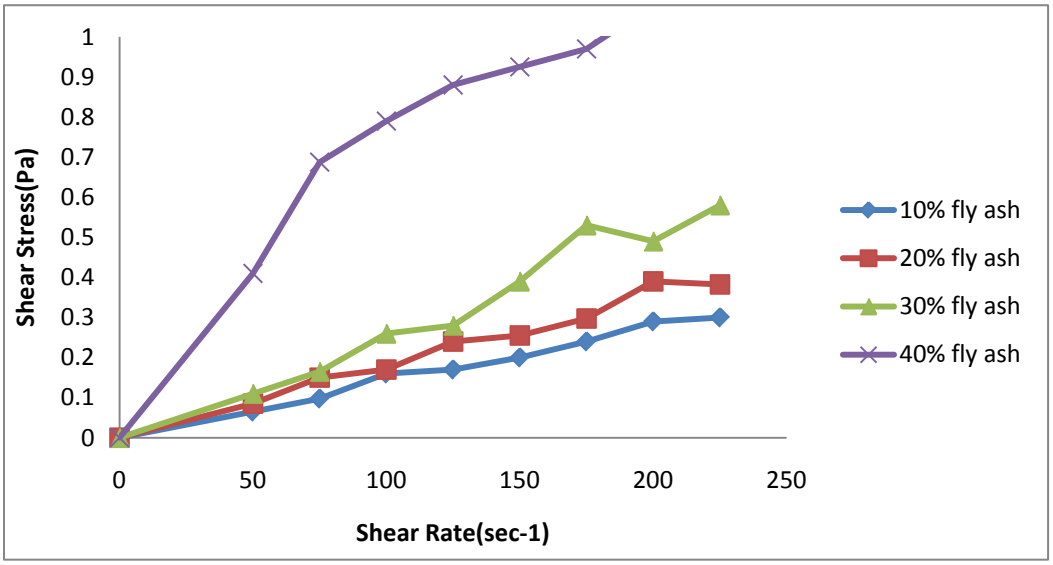

Figure 3.7 Shear Stress Vs Shear Rate Plot of Fly Ash

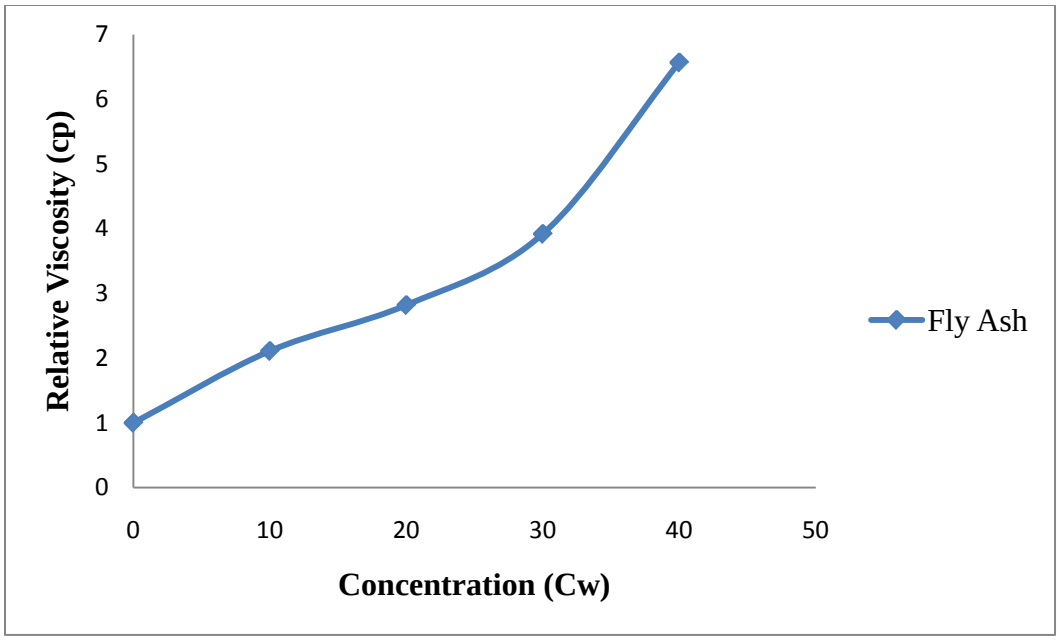

Figure 3.8 Relative Viscosity Vs Concentration Plot

3.5) pH VALUE:

pH meter was used to determine pH value of fly ash slurry for any given solid concentration. The electrode of the pH meter was first moistened with tap water and then calibrated with a buffer solution of a known Ph value.

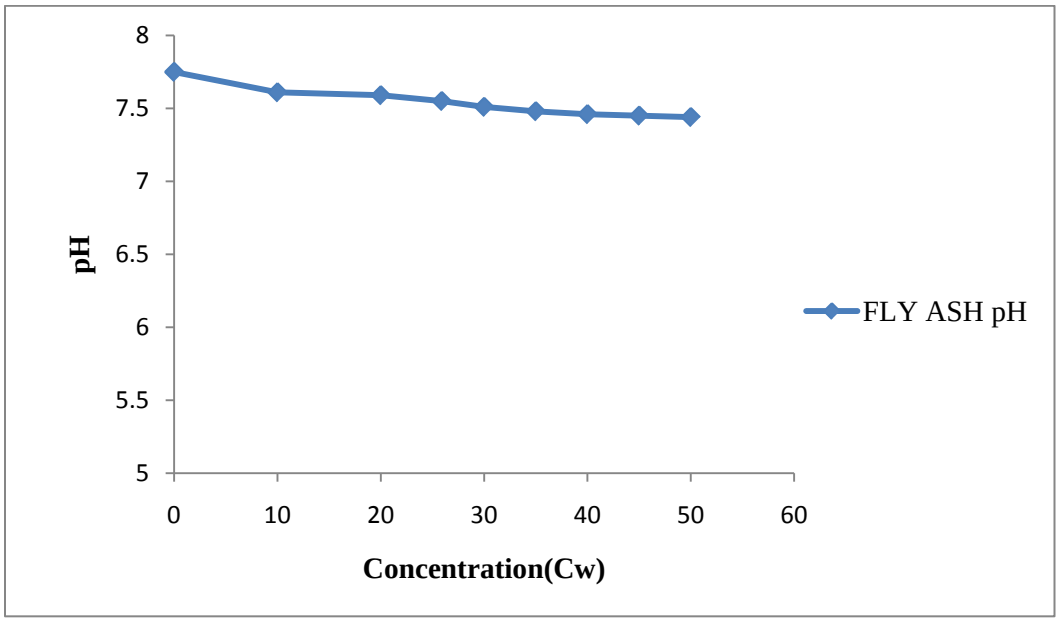

Figure 3.9 pH value Vs Concentration plot of Fly Ash

It is cleaned by rinsing vigorously with distilled water and then immersed in the slurry sample whose pH value was to be determined. The pH suspension was read on the digital display unit when equilibrium value was reached. The experimental results of pH value of fly ash are shown in table 1.5 (Annexure III).

In this test first prepare 7 pH or 4 pH solution dissolve 1 buffer tablet in 100 ml of distilled water. Insert the probe pH meter in the solution and wait for 5 minutes till readings get stabilized. If reading is not equivalent to the pH of solution, then change the control and make the readings equivalent to the pH value of solution. Remove the probe and dip into the distilled water beaker and then dip into the solution or slurry of which PH value is to be determined. Wait for 5 minutes till the reading is stabilized.

CHAPTER 4

STUDY OF PROPERTIES OF MATERIALS

Steel based materials that are largely used in pumps, turbines and pipelines undergo erosion wear. Erosion wear is also serious problem for the fly ash handling system of a power plant. It reduces the service life of components of ash handling system. So it is needed to improve the erosion resistant properties of these materials. Various methods such as surface modifications, coating and deposition of paint layers are applied to increase the surface wear resistant properties.

In the present work, an attempt has been made to strengthen the surface erosion wear resistant properties of 13Cr4Ni steel by depositing Al_2O_3 and Cr_2O_3 coatings to the same.

4.1) BASE MATERIAL:

In present erosion wear study, 13Cr-4Ni steel used as base material. This material (termed as 13/4 steel) is currently being used for fabrication of pumps for different applications and under water parts in hydroelectric projects because its nickel content, associated with low carbon ensures better erosion resistance, weldability, ductility, impact resistance and fatigue resistance properties. This steel alloy has also good corrosion resistance to fresh water and performs well under erosion-corrosion phenomena. The alloy is specially designed for all applications requiring high mechanical properties combined with high toughness and may be used in erosive - corrosive conditions. Typical applications are shafts or pump impellers, particularly for hydraulic applications.

4.2) PROPERTIES OF BASE MATERIAL:

The various properties of 13Cr4Ni stainless steel has been discussed below:

4.2.1) Chemical Composition:

The chemical composition of 13Cr4Ni samples were determined by the spectrometer analysis. A spectrometer (also known as spectrophotometer, spectrograph or spectroscope) is a device that used to measure the chemical composition of ferrous materials. The chemical composition is measured by the light intensity produced by arc. A spectrometer is used

in spectroscopy for producing spectral lines and measuring their wavelengths and intensities. Spectrometer instruments that operate over a very wide range of wavelengths, from gamma rays and X-rays into the far infrared. Figure 4.1, showing the spectrometer.

Figure 4.1 Spectrometer

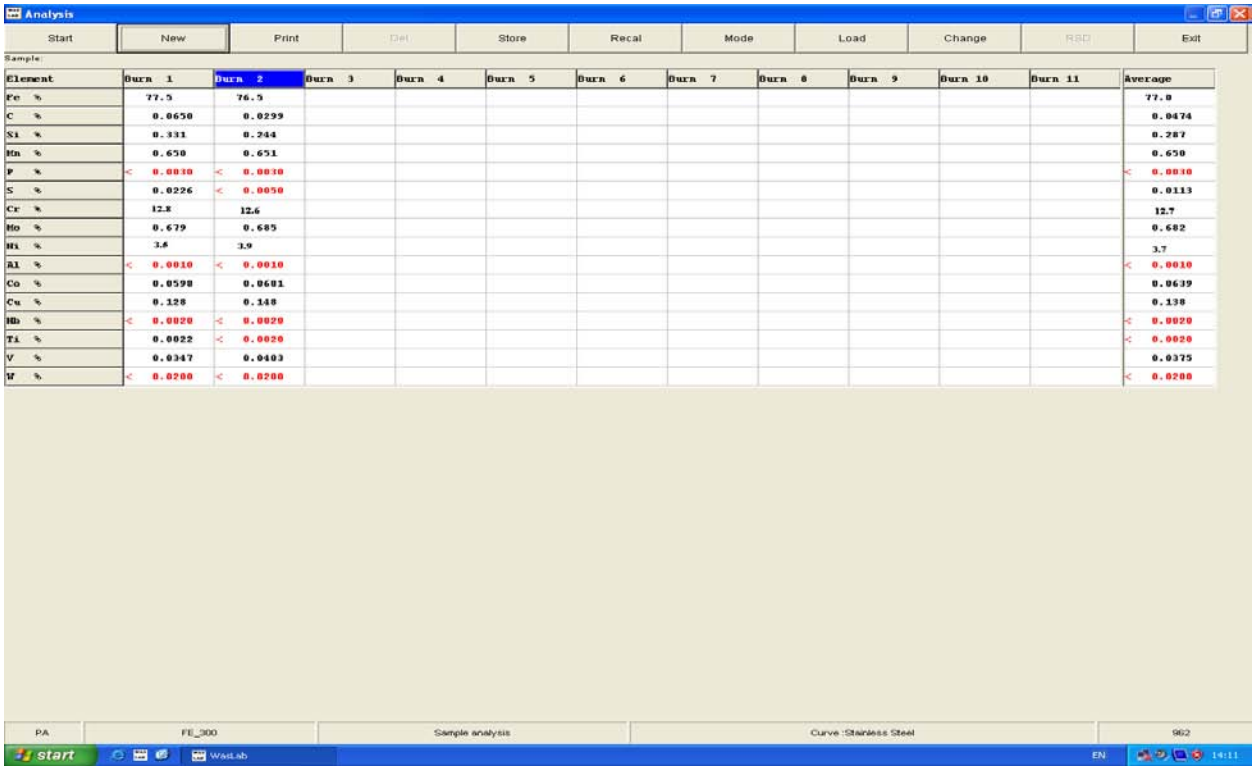

Figure 4.2 Chemical Composition of 13Cr4Ni Steel

Table 4.1 Main Chemical Composition of 13Cr4Ni Steel:

Components	Percentage composition
Cr	12.7
Ni	3.7
C	0.07
Si	0.28
Mn	0.65
Mo	0.68
Fe	78

4.2.2) Micro Hardness:

Micro hardness of both type of specimens (uncoated and coated) was determined by using micro hardness tester (as shown in figure 4.2). A load of 300gm was applied by using a calibration

Figure 4.3 Micro Hardness Tester

distance of 50 units in quantinet and VHN values were determined. During the load application dwell time used was 25 seconds.

Table 4.2 Specimens Micro Hardness:

Base Material	Coating	Hardness (VHN)
13Cr4Ni Stainless Steel	————	332
13Cr4Ni Stainless Steel	Al_2O_3	1140
13Cr4Ni Stainless Steel	Cr_2O_3	1320

4.3) COATINGS:

To improve the erosion wear resistance of base material 13Cr4Ni stainless steel cotings of aluminium oxide (Al_2O_3) and chromium oxide (Cr_2O_3) powders has done using High Velocity Oxygen Fuel (HVOF) method. The substrate material is coated at Metallizing Equipment Company Pvt. Ltd. Jodhpur.

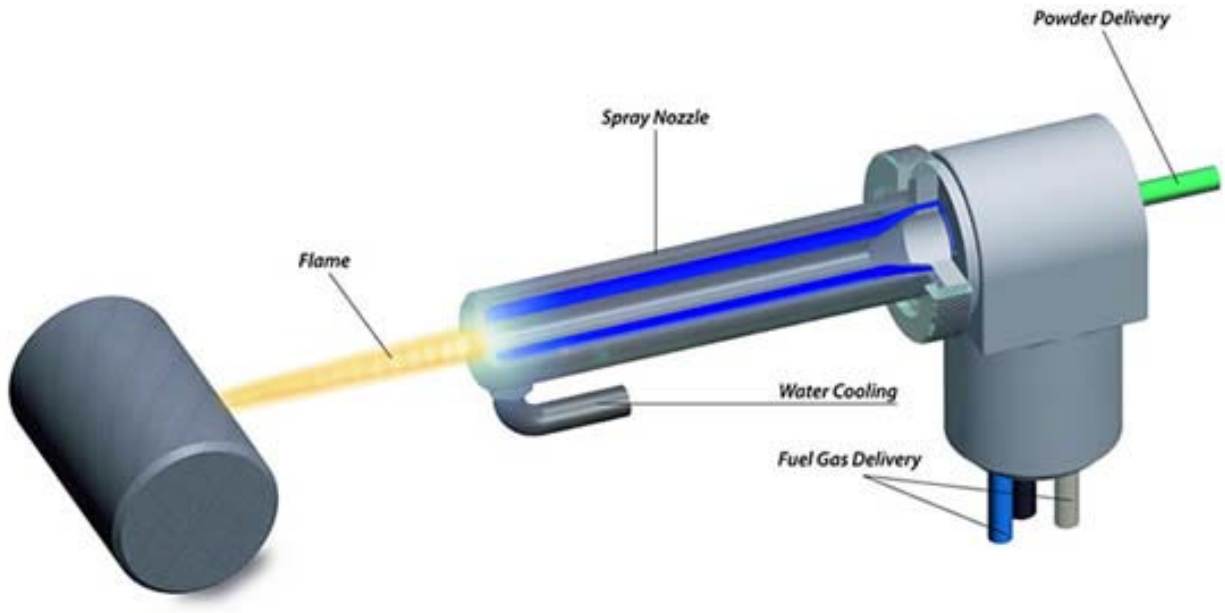

Figure 4.4 Schematic Diagram of HVOF Coating Gun

In High Velocity Oxygen Fuel (HVOF) method, a mixture of gaseous or liquid fuel and oxygen is fed into a combustion chamber, where they are ignited and combusted continuously. The

resultant hot gas at apressure close to 1 MPa emanates through a converging–diverging nozzle and travels through a straight section. The fuels can be gases (hydrogen, methane, etc.) or liquids (kerosene, etc.). The figure 4.4 showing schematic diagram the coating gun generally used for the high velocity oxy fuel thermal coatings.

This process produces extremely high spray velocity. The jet velocity at the exit of the barrel (>1000 m/s) exceeds the speed of sound. For this coating work feed stock of Al_2O_3 and Cr_2O_3 powders is injected into the gas stream, which accelerates the powder up to 800 m/s. Powders fed into the HVOF combustion chamber under high pressure. The stream of hot gas and powder is directed towards the surface to be coated. The powder partially melts in the stream, and deposits upon the 13Cr4Ni stainless steel sheet. HVOF coatings are very dense, strong, high bond strength and show low residual tensile stress.

4.3.1) Aluminium Oxide:

Aluminium oxide is an amphoteric oxide with the chemical formula Al_2O_3. It is commonly referred to as alumina, or corundum in its crystalline form, as well as many other names, reflecting its widespread occurrence in nature and industry. Its most significant use is in the production of aluminium metal, although it is also used as an abrasive owing to its hardness and as a refractory material owing to its high melting point. Aluminum oxide possesses strong ionic interatomic bonding giving rise to it's desirable material characteristics. It can exist in several crystalline phases which all revert to the most stable hexagonal alpha phase at elevated temperatures. Some of the key properties of aluminium oxide are hard, wear-resistant, excellent dielectric properties from DC to GHz frequencies, resists strong acid and alkali attack at elevated temperatures, good thermal conductivity, excellent size and shape capability,high strength and stiffness.

Alumina is the strongest and stiffest of the oxide ceramics. Its high hardness, excellent dielectric properties, refractoriness and good thermal properties make it the material of choice for a wide range of applications. Because of these enormous properties aluminium oxide is largely used in gas tubes, wear pads, seal rings, high temperature electrical insulators, high voltage insulators, furnace liner tubes, thread and wire guides, electronic substrates,ballistic armor, abrasion

resistant tube and elbow liners, thermometry sensors, laboratory instrument tubes and sample holders, instrumentation parts for thermal property test machines and grinding media.

High purity alumina is usable in both oxidizing and reducing atmospheres to 1925°C. Weight loss in vacuum ranges from 10^{-7} to 10^{-6} g/cm^2.sec over a temperature range of 1700° to 2000°C. It resists attack by all gases except wet fluorine and is resistant to all common reagents. The composition of the ceramic body can be changed to enhance particular desirable material characteristics.

High Hardness of aluminium oxide makes it suitable for use as an erosion resistant coating on various components of slurry transport system and component in cutting tools. The table 4.1 showing the properties of aluminium oxide powder.

Table 4.3 Properties of Aluminium Oxide Powder

Composition	Sio_2 – 0.1% max Fe_2O_3 – 0.05 % max Na_2O – 0.3 % max
Powder Size (µm)	- 45 + 22
Apparent Density	1.8
Coating Thickness (µm)	200 ± 10
Hardness (Kg/mm^2)	1150
Compressive Strength (MPa)	2000

4.3.2) Chromium Oxide:

Chromium oxide is the inorganic compound of the formula Cr_2O_3. It is one of principal oxides of chromium and is used as a pigment. In nature, it occurs as the rare mineral eskolaite. It has a complex refractive index of 2.24 - 0.07i near 700 nm and a transmittance range from below 1.2 µm to 10 µm; however, these optical constants are strongly affected by the substrate temperature

during deposition. Chromium oxide is the hardest oxide that also exhibits low friction coefficient, high wear and corrosion resistance, and good optical and adiabatic characteristics.

These properties allow it to be used as a protective coating in tribological and microelectronic applications and as an adiabatic material in aeronautic and space fields. Cr_2O_3 thin films are quite hard and have anti-corrosion and anti-wear properties; hence, they are used as buffer layers to improve erosion and adhesion or as oxidation-resistant coatings.

Table 4.4 Properties of Chromium Oxide Powder

Composition	Cr = 68.42% O = 31.58%
Powder Size (µm)	- 35 + 22
Specific Gravity	5.22
Coating Thickness (µm)	200 $\pm$ 10
Hardness (Kg/mm^2)	1320
Compressive Strength (MPa)	2200

CHAPTER 5

EXPERIMENTATION

Erosion wear of 13Ni4Cr steel with and without coatings of aluminium oxide and chromium oxide were performed on a jet erosion tester situated at Baba Banda Singh Bahadur Engineering collage Fatehgarh Sahib, Punjab. The fly ash and water mixture is used as slurry medium. The fly ash collected from the Guru Gobind Singh Super Thermal power plant, Ropar.

5.1) EXPERIMENTAL SETUP:

The jet erosion tester (figure 4.1) consists of a centrifugal pump, conical tank, nozzle, specimen holder, valves and flow meter. The centrifugal pump is driven by a 7.5 HP, 1400 rpm electric motor having a capacity of max pressure 13.5 bar at a discharge of 240L/min. Slurry available in conical tank is sucked through a 100mm GI pipe with help of pump and delivered to the nozzle through 25 mm pipe having control valves and electromagnetic flow meter located at upstream. Slurry is re-circulated during test. The mechanical action of slurry pump increase the temperature of slurry to a certain level and thereafter it remains constant. The flow rate of the slurry is controlled with help of main valve and bypass regulator valve between delivery side and nozzle. The tank is rectangular tapered having size 650×650 mm at top which converges to 100×100 mm at the bottom through a length of 700 mm is used to store the slurry. A mesh is provided in the bottom of the tank to avoid the object from falling into the tank and get struck inside the pipeline.

Slurry flowing through the pump at high pressure is converted into high velocity stream while passing through the converging section of the nozzle, which is 125mm long, and having diameter of 8 mm. The standoff distance between the nozzle and specimen can be varied from 25mm to 90mm. The slurry falls back into the tank after striking to specimen. The holder is located on the top of tank enclosed in a casing made of steel angle and fitted with fiber sheet, to facilitate the removal and clamping of the specimen. The electronic magnetic flow meter (Elmag-200M) arranged (as shown in figure 4.1) in between control valves and nozzle, is equipped with digital display and contains PTEF coated liner through which the slurry flows and discharge is calculated, when a conductive fluid passes through magnetic field (applied) a voltage is induced

in an electrically conductive body which is proportional to the mean flow velocity according to Faraday's law of induction.

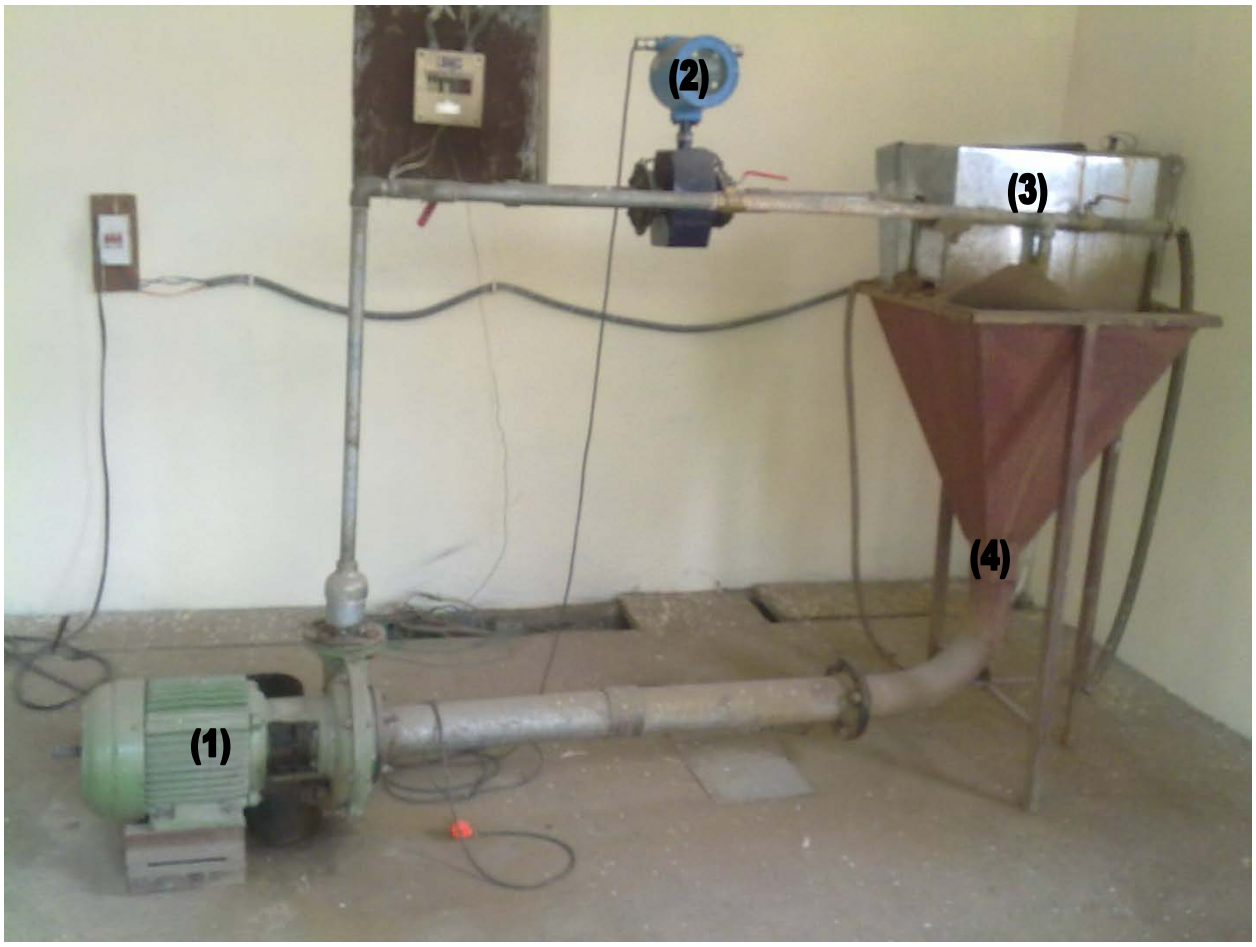

Figure 5.1 Jet Erosion Tester

(1) Centrifugal pump

(2) Electronic magnetic flow meter

(3) Nozzle and Holder assembly

(4) Conical Tank

5.2) WORKING OF JET EROSION TESTER:

In jet erosion testing a high velocity jet strikes a flat specimen at some adjustable angle. In this test, the amount of material removed is determined by the weight loss. The material, which accumulates on the specimen surface, interferes with the incoming particle. The weight loss of the specimen corresponds to the average erosion over the surface.

Jet erosion tester has been developed to investigate the effect of different parameters particularly the impact angle under controlled environment. In jet erosion tester, a circular jet of solid–liquid mixture strikes at the wear specimen fixed in a fixture, which can be oriented at any angle with respect to the former. Generally, a pump is used to drive water at high pressure and the solid particles are being sucked through an injector. The mixing of the solid–liquid is formed in the mixing chamber before the jet comes out through a nozzle.

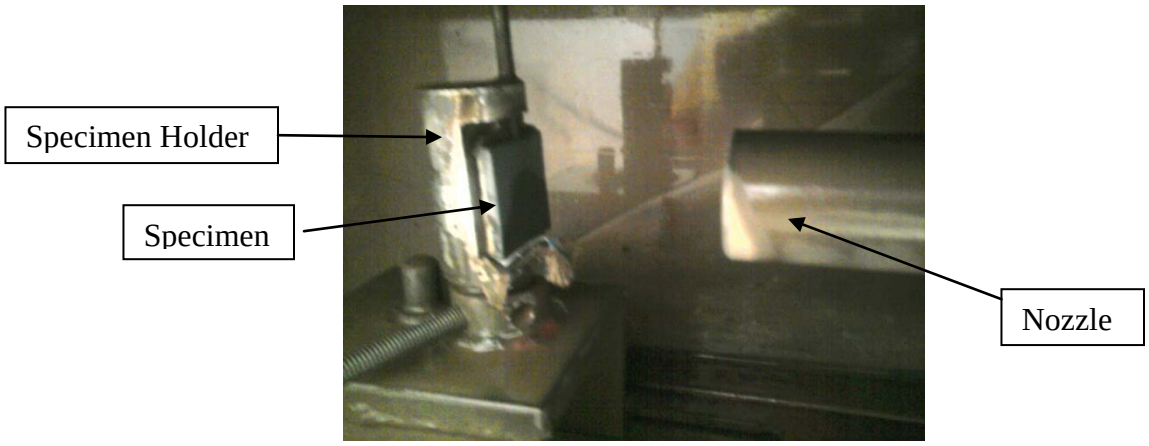

Figure 5.2 Specimen Holder and Nozzle

In most generalize way, three typical erosion test rig types can be considered on the basis of relative motion between mixture and specimen. They are

1. Jet/ Nozzle type
2. Rotating disc/Arm type and
3. Centrifugal accelerator type.

Jet type of test rig selected for experimental investigation of erosion in this research was developed as a part of master level project work at B.B.S.B.E.C, Fatehgarh Sahib. The reason for the selection of this type of test rig was also to facilitate the study of the effect of different parameters (impact angle etc.) and to enhance the knowledge of the erosion mechanism, which

otherwise had not been possible in other type of test rig available. Other reason for the selection of jet type of test rig compared to other rotating equipment and its advantages are:

- Test cycle time in jet type of test rig.
- The erosion of material foe different impingement angles is possible.
- Control of variable like velocity and concentration is easy and several test points are possible.
- Very high velocities can be achieved compared to other available test rigs.

This is very much similar to the practical situation of Pelton turbine and low impact angle tests resemble flow in reaction turbine components.

5.3) SAMPLES PREPARATION:

The steel mostly used in slurry transportation system i.e. 13Cr4Ni is to be used for erosion wear testing purpose. By using power hacksaw, The samples of 5 mm thickness are cut from a long bar of cross- sectional area $40 \times 40\ mm$. Surface grinder is used to finish the surface of each sample. As per the requirement the coating of aluminium oxide and chromium oxide is to be done on the sample by high velocity oxy fuel (HVOF) thermal spray technique. The samples were used from both sides for testing for coated and non-coated materials.

(a) Uncoated 13Cr4Ni Steel **(b) Cr_2O_3 Coated Steel** **(c) Al_2O_3 Coated Steel**

Figure 5.3 Samples Images

The coating of aluminium oxide and chromium oxide powders over the samples is done with HVOF technique, at Metalizing Equipments company pvt ltd, Jodhpur. Abrasive blasting is done on the samples by alumina grits before applying the coatings. Grit blasting of samples is necessary before applying the coating so as to supplement the adhesion of the coatings to the surface of sample.

5.4) COATING PROCEDURE:

As earlier mentioned that HVOF thermal coating method was used for coating the 13Cr4Ni steel samples at Metalizing Equipment Company, Jodhpur. In this coating process, the fuel (Gas/Liquid) along with oxygen is introduced into the combustion chamber where it burnt and high temperature pressure combustion products exhausted through nozzle. The powder to be coated is supplied along with this superheated high velocity stream.

Figure 5.4 High Velocity Oxy-Fuel (HVOF) Coating Machine.

The powder, in this superheated high velocity stream get melted and deposited on sample surface. In this coating process LPG was used as fuel (Gas) and nitrogen gas was used as a carrier gas to circulate/supply the powder along with superheated, high velocity stream. The figure 5.1 showing the HVOF coating machine situated at Metalizing Equipment Company Pvt Ltd, Jodhpur.

In this process, a very high temperature of 3000+℃ achieved through fuel gas combustion. A very high velocity of about 800 m/s was used during the process. The indicator (in figure 5.1) in the control panel indicates the flow of fuel oxygen and carrier gas. The powder was filled in the black box just below the indicators and above stop/start button.

5.5) EXPERIMENTAL PROCEDURE:

Erosion wear experiments performed through a sequence of steps, in which most of the observations recorded manually and graphs plotted accordingly. The mass loss of the specimen after each test is the measure of erosion wear. The sequence of steps of experimental procedure is as given below:

1. The wear sample is rinsed in acetone and clean with emery paper.
2. Dry the sample properly.
3. Weighing the specimen (initial weight).
4. Fix the sample in holder.
5. Set the holder at a certain angle.
6. Weight the required amount of fly ash as per concentration of slurry.
7. Mixing the proper amount of water and fly ash in tank.
8. Start the pump.
9. Control the slurry flow rate by mean of flow meter and a by-pass valve to obtain desired value of velocity
10. Perform the test for different flow rate, impact angle and required time interval.
11. Unclamp the specimen from specimen holder
12. Cleaning specimen with acetone and drying it.
13. Weighing the specimen after erosion to measure the mass loss
14. For further observations repeat the procedure steps from 4 to 13 as per requirement

Table 5.1 Experimentation Parameters:

Dimensions of Specimen	40 mm × 40 mm × 5 mm
Flow Rate	Maximum 3.5 lit/sec
Angle	30°,60° and 90°
Slurry Concentration	20% by weight
Fly Ash particle Size	50 -350 micron
Time	Maximum 4 hours
Nozzle Diameter	8 mm
Stand Off Distance	45 mm

CHAPTER 6

RESULTS AND DISCUSSIONS

The erosion wear tests of coated and uncoated 13Cr4Ni steel were performed at various ash particles impingement angles, flow rate and time. The particle size of the fly ash used in this experimentation was varied between 50 and 350 µm and 20% slurry concentration was taken. The ash was collected from chimney of Guru Gobind Singh Super thermal power plant, Ropar. The results of wear with all above mentioned parameters will be discuss in this chapter.

6.1) SCANNING ELECTRON MICROSCOPE ANALYSIS:

A scanning electron microscope (SEM) is a type of electron microscope that images a sample by scanning it with a high-energy beam of electrons. The electrons interact with the atoms that make up the sample producing signals that contain information about the sample's surface topography, composition, and other properties such as electrical conductivity. The samples of material used for erosion purpose was examined with help of scanning electron microscope with aim to visualize change in microstructure in order to know the mechanism of erosion. All the samples analyzed were subjected to maximum velocity and impact angle of 90°.

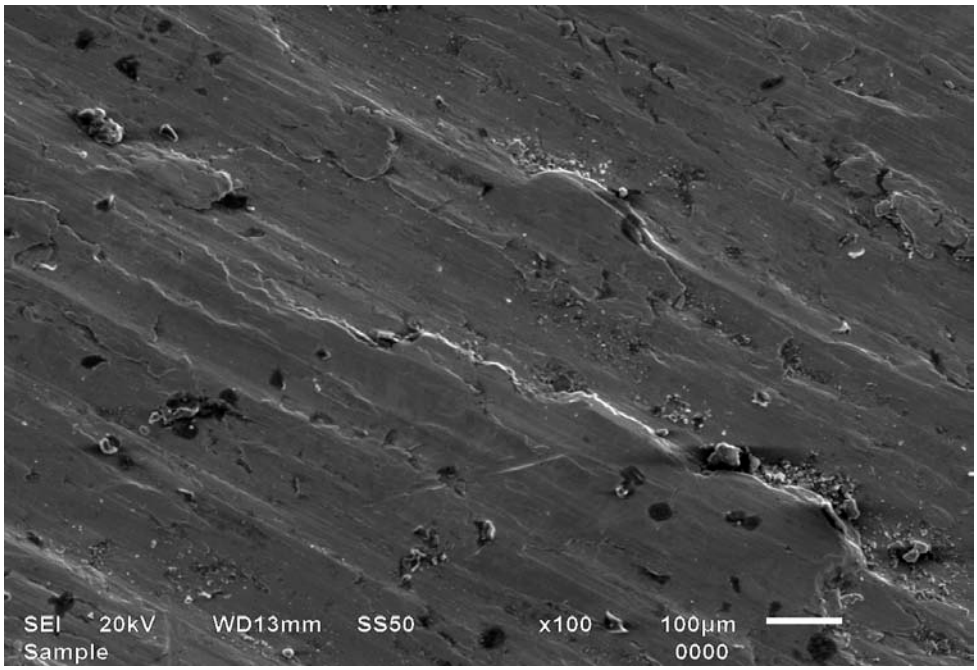

Figure 6.1 (a) SEM of 13Cr4Ni Steel Before Wear

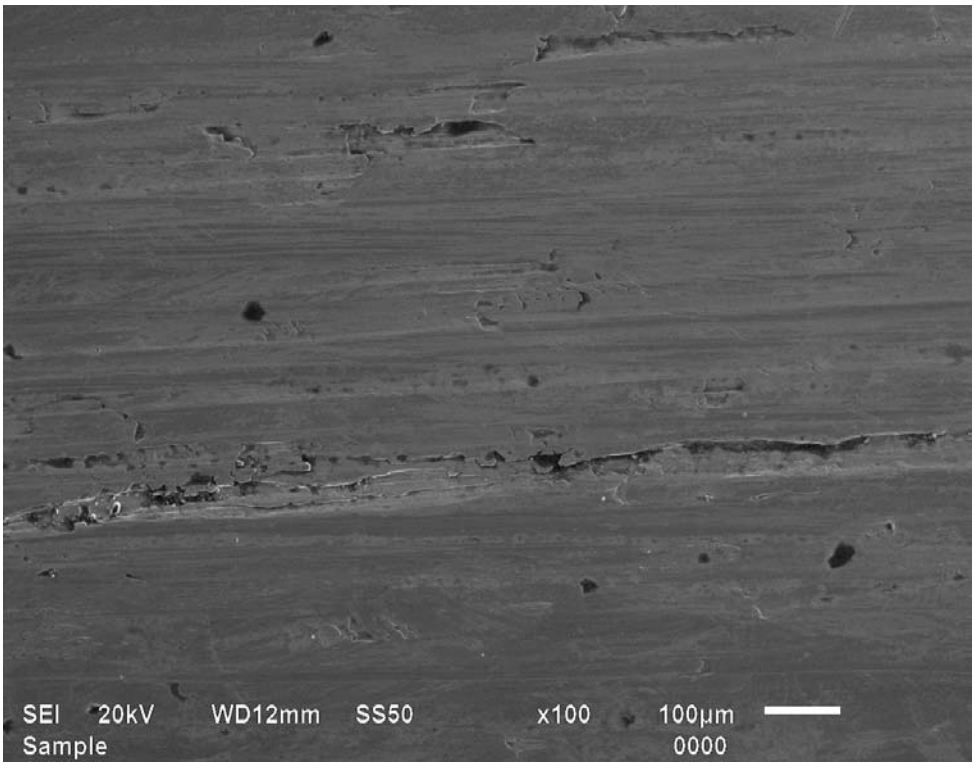

Figure 6.1 (b) SEM of 13Cr4Ni Steel After Wear

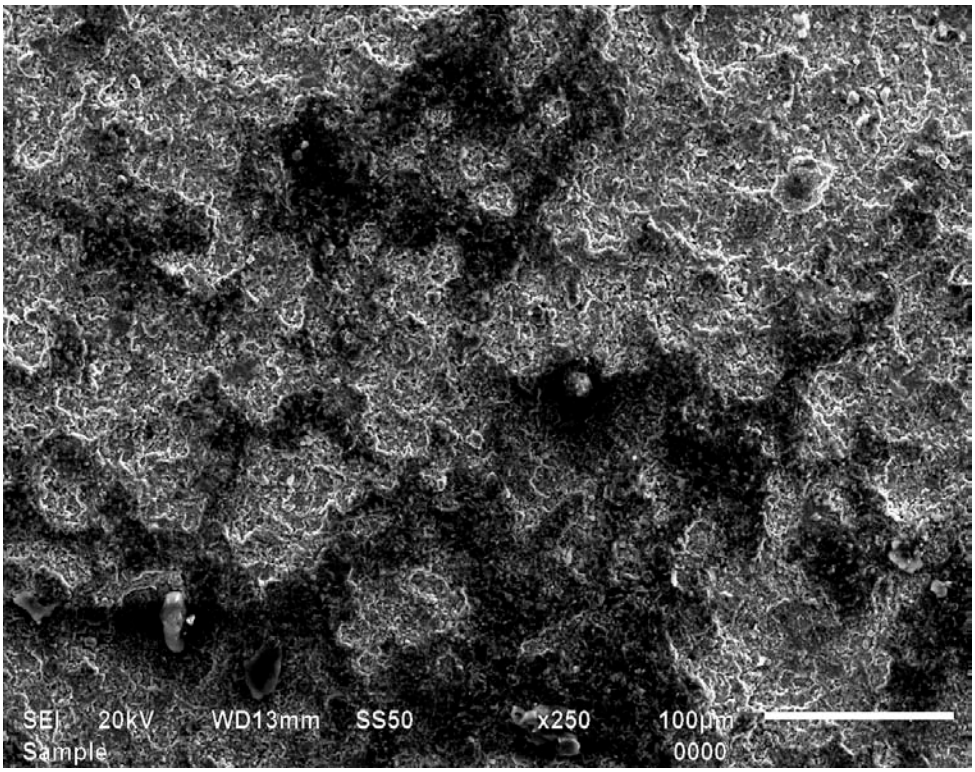

Figure 6.2 (a) SEM of Al_2O_3 Coating Befor Wear

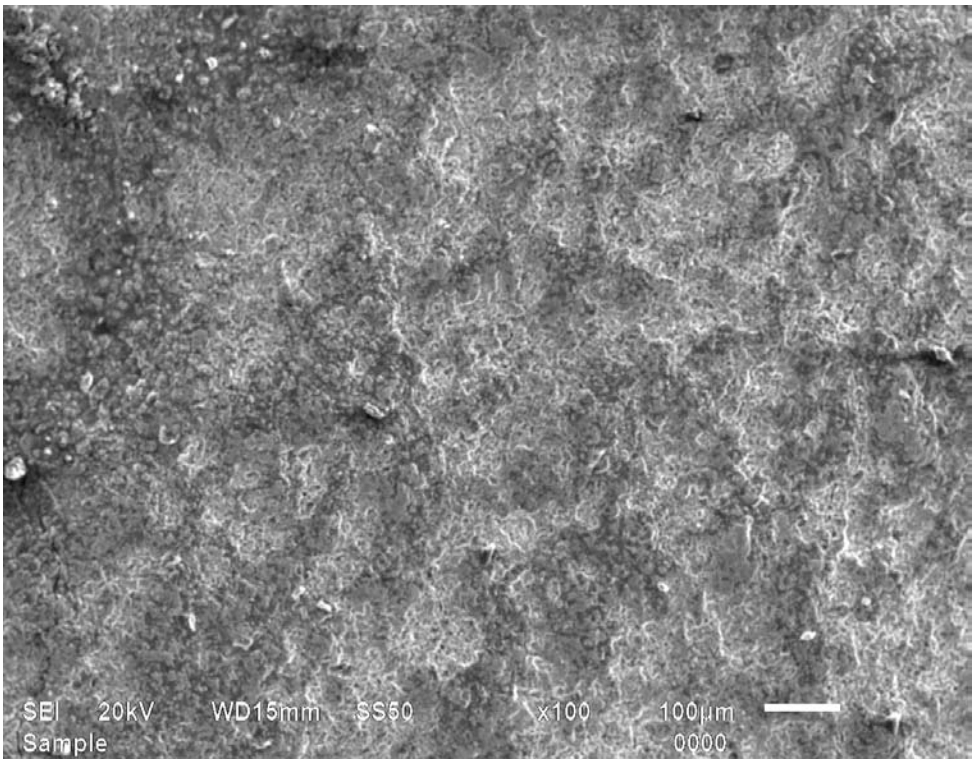

Figure 6.2 (b) SEM of Al_2O_3 Coating After Wear

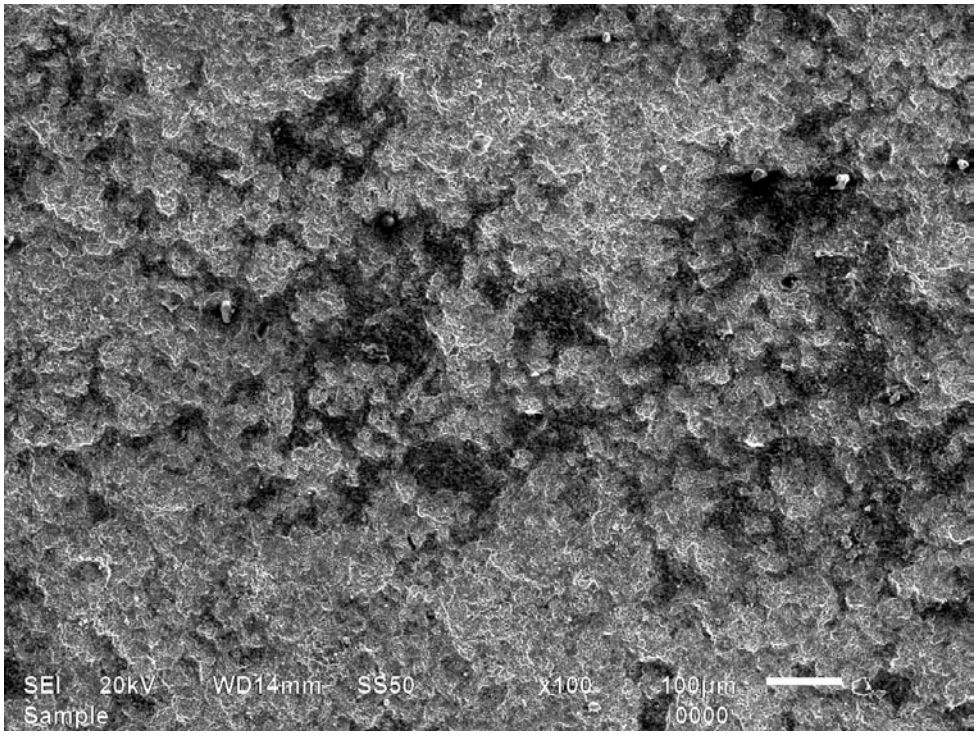

Figure 6.3 (a) SEM of Cr_2O_3 Coating Befor Wear

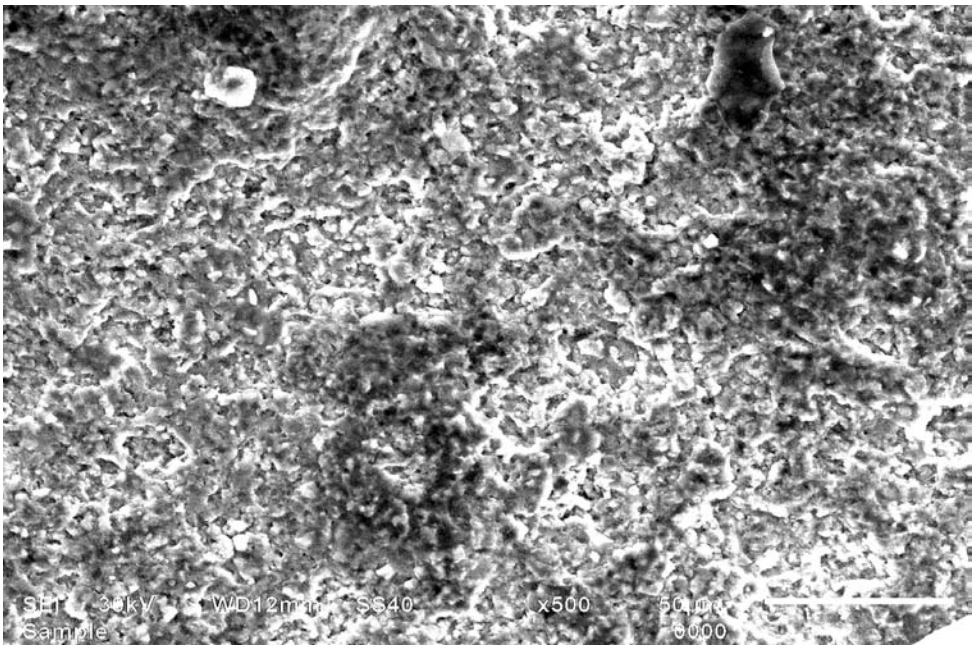

Figure 6.3 (b) SEM of Cr_2O_3 Coating After Wear

6.2) EFFECT OF IMPACT ANGLE ON EROSION WEAR:

The angle at which fly ash particles impacted at sample surface has a significant effect on erosion wear and its mechanism.

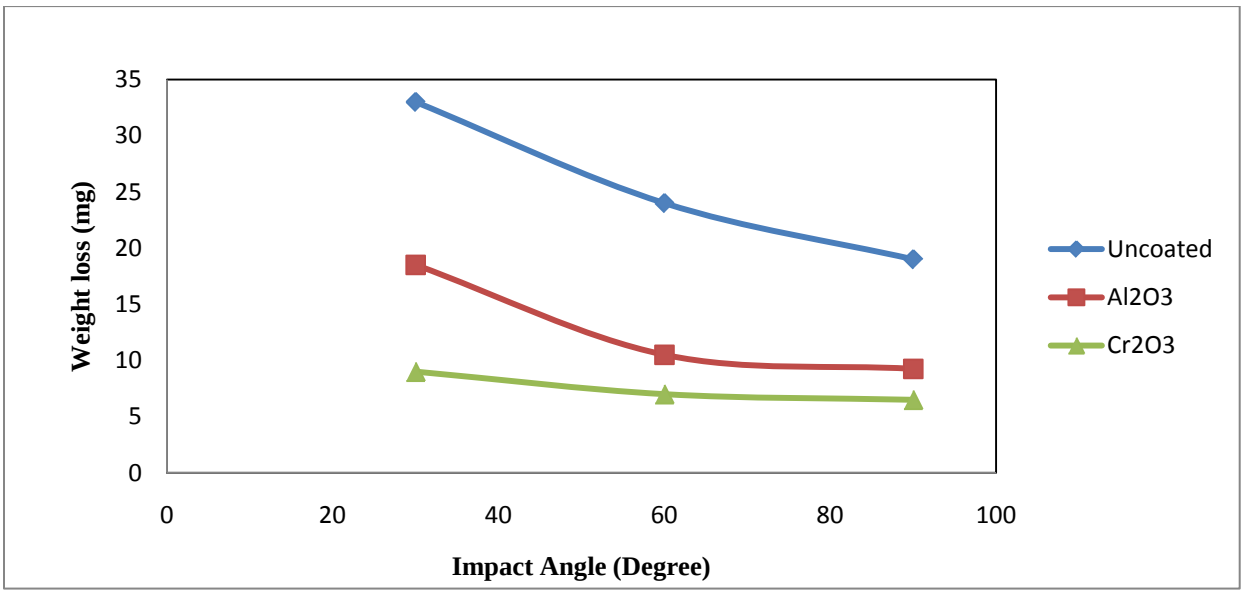

Figure 6.4 Variation in weight loss with respect to impact angle at 1.75 lit/sec flow rate.

Figure 6.4 and table 1.6 in annexure IV shows the effect of impact angle on erosion wear of 13Cr4Ni steel, Al_2O_3 and Cr_2O_3 coatings. The erosion wear of different samples evaluated at three different impact angles 30°, 60° and 90°. Among all the three impact angles, 30° impact angle shows the maximum erosion wear and impact angle 90° shows minimum erosion wear. Higher erosion wear at 30^0 impact angle indicates that 13Cr4Ni steel is ductile material.

Higher erosion wear at 30° is because of the presence of austenitic phase. At lower angle micro cutting and ploughing mechanisms are predominant. The tangential component of velocity is responsible for higher erosion wear at lower angles. At higher angles, crack intimation is more predominant and responsible for erosion wear of materials. At higher angle, the normal component of velocity is responsible for erosion wear. The plastic deformation of surface and work hardening are the phenomenon, which occurs at higher angles and leads to reduction in weight loss. Erosion at 90^0 is because of normal component of velocity, causing fatigue and fracture of grain boundaries.

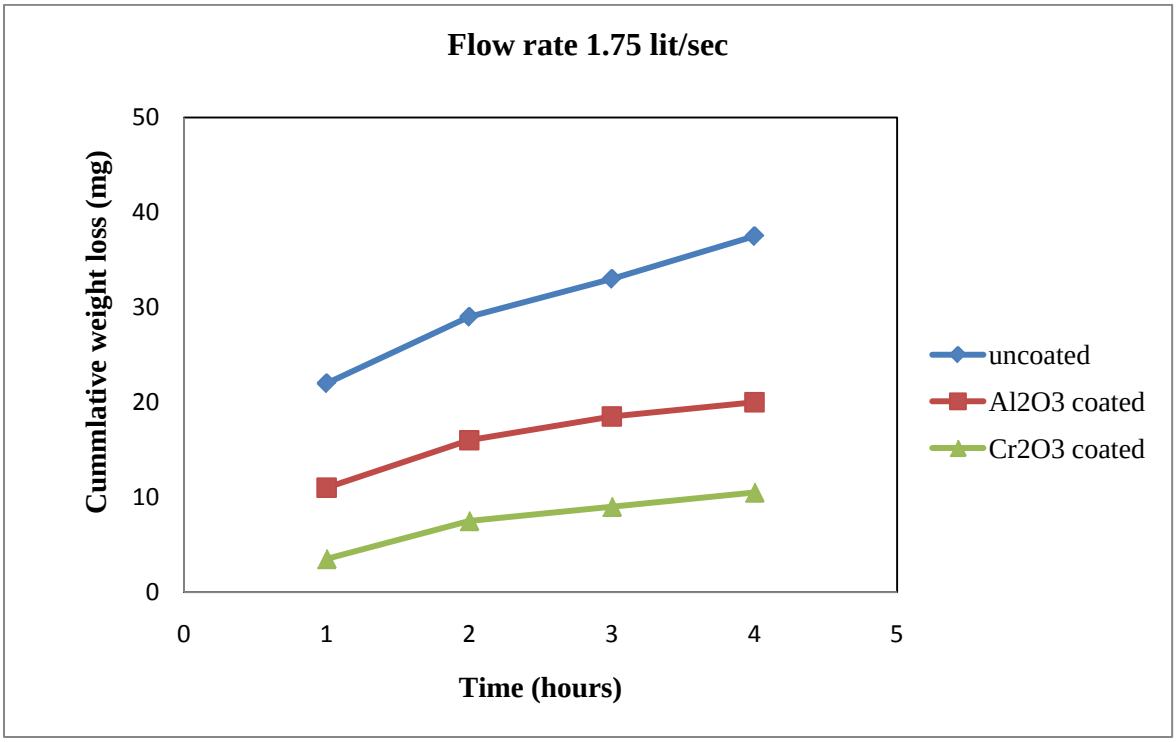

Figure 6.5 Variation in cumulative weight loss with respect to time at 30° impact angle.

In figure 6.4 (table 1.6 in annexure IV) as the impact angle decreases the weight loss increases. Both the coatings Al_2O_3 and Cr_2O_3 show better performance than 13Cr4Ni steel. The coating of

Cr_2O_3 shows the maximum erosion wear resistance among Al_2O_3 coating and bare 13Cr4Ni steel samples.The bond strength and hardness of chromium oxide coating is higher than aluminium oxide. The difference in weight loss at lower angle is very high as compared to higher angles.

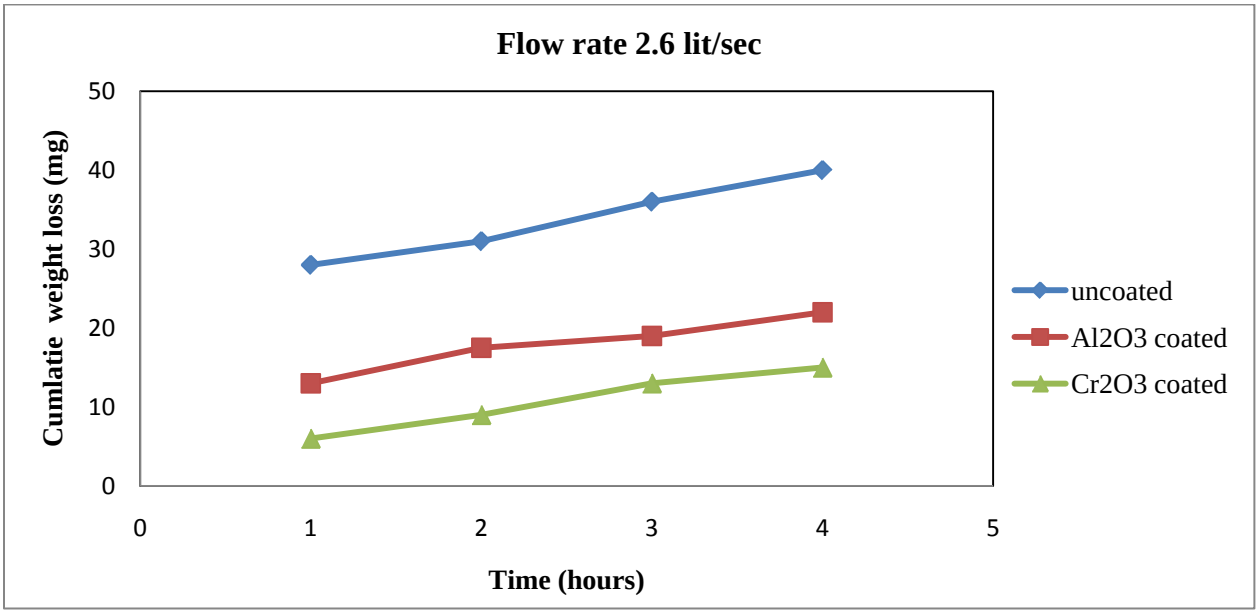

Figure 6.6 Variation in cumulative weight loss with respect to time at 30° impact angle

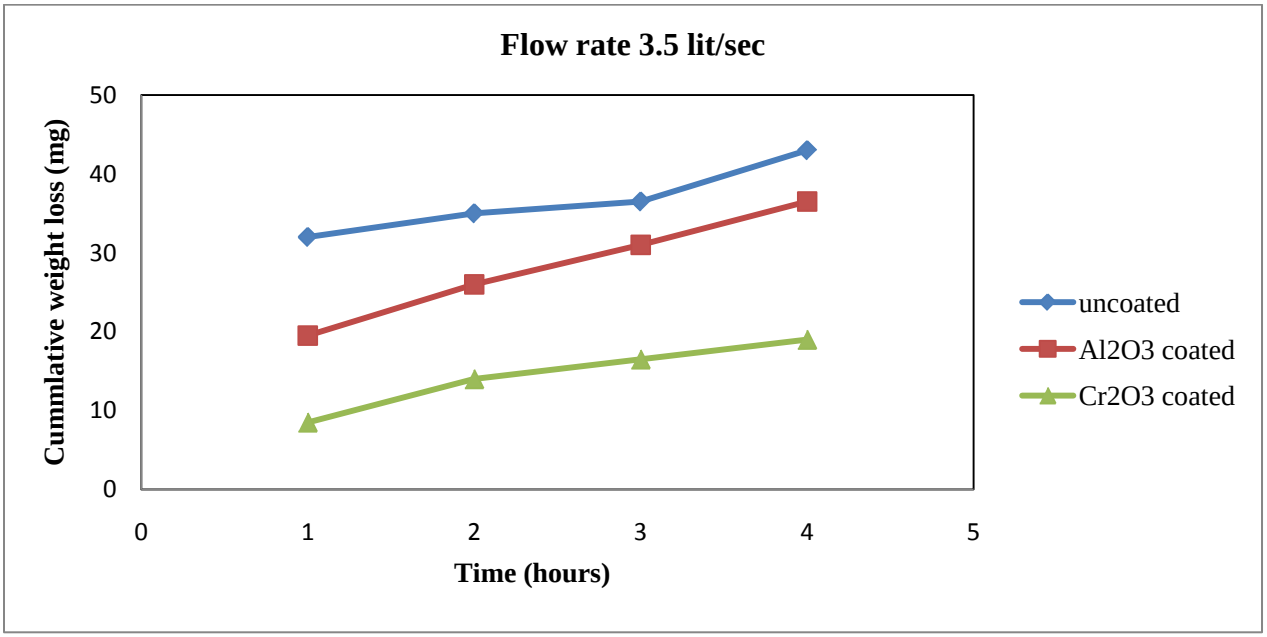

Figure 6.7 Variation in cumulative weight loss with respect to time at 30° impact angle

At lower angles, the effect of bond strength of coating is more than at normal angles. A slight decrease in weight loss is observed when angle is changed from 30^0 to 60^0. The variations in cumulative weight loss with respect to time at different impact angles and flow rate are shown in figures from 6.5 to 6.13 and tables 1.7 to 1.9 in annexure IV.

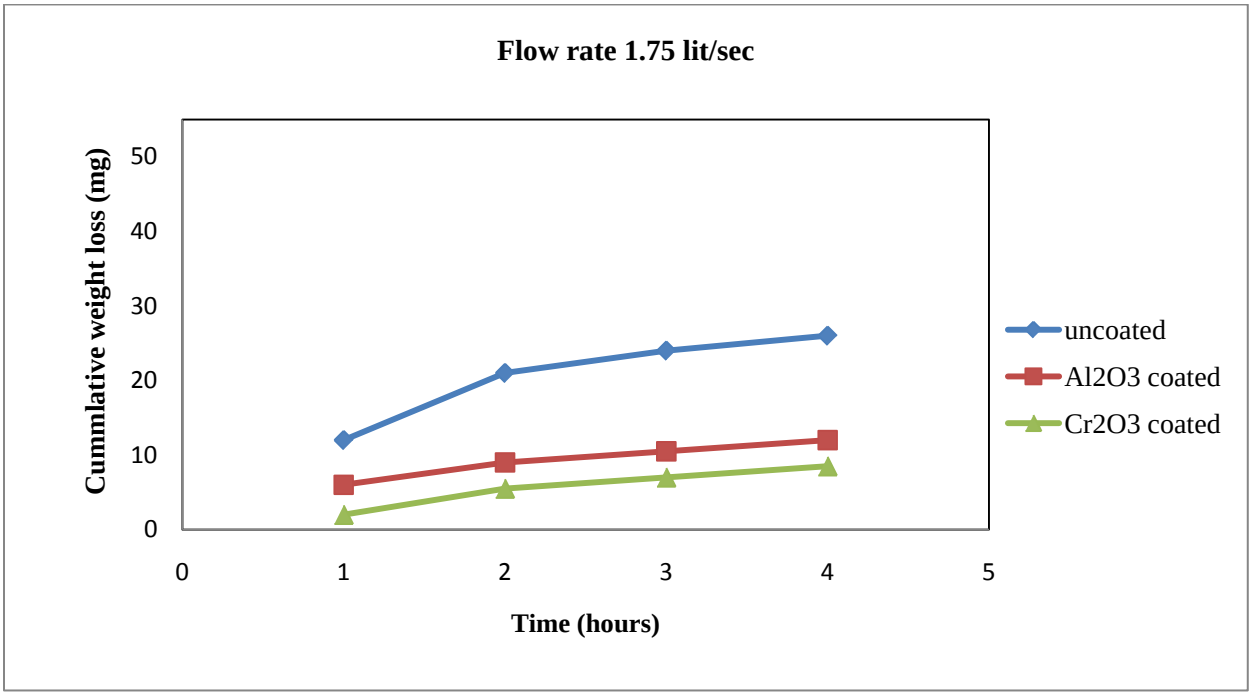

Figure 6.8 Variation in cumulative weight loss with respect to time at 60° impact angle

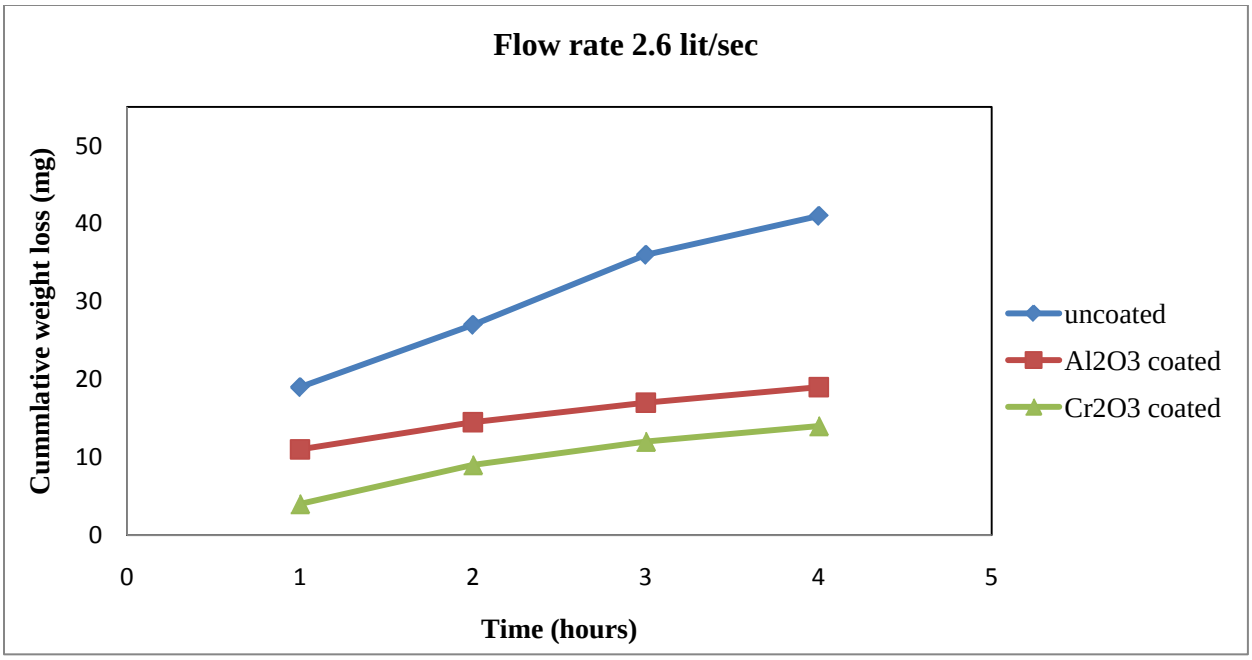

Figure 6.9 Variation in cumulative weight loss with respect to time at 60° impact angle

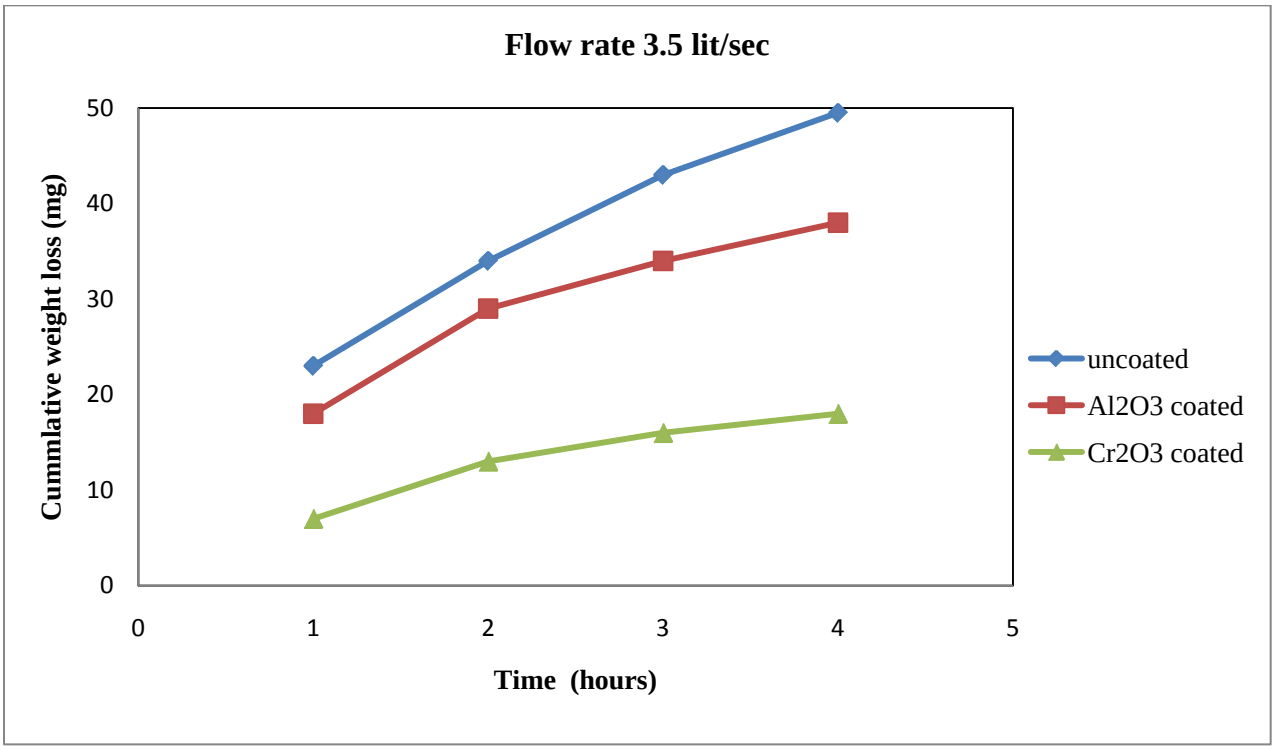

Figure 6.10 Variation in cumulative weight loss with respect to time at 60° impact angle

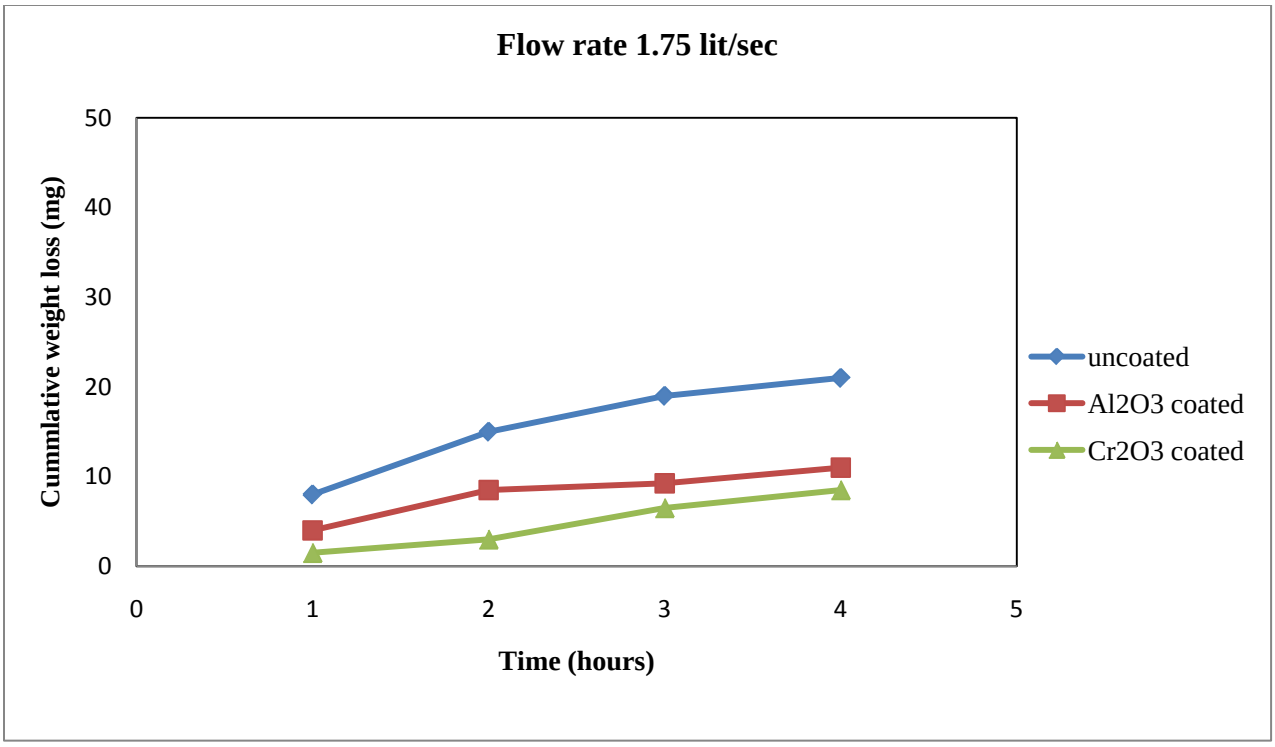

Figure 6.11 Variation in cumulative weight loss with respect to time at 90° impact angle

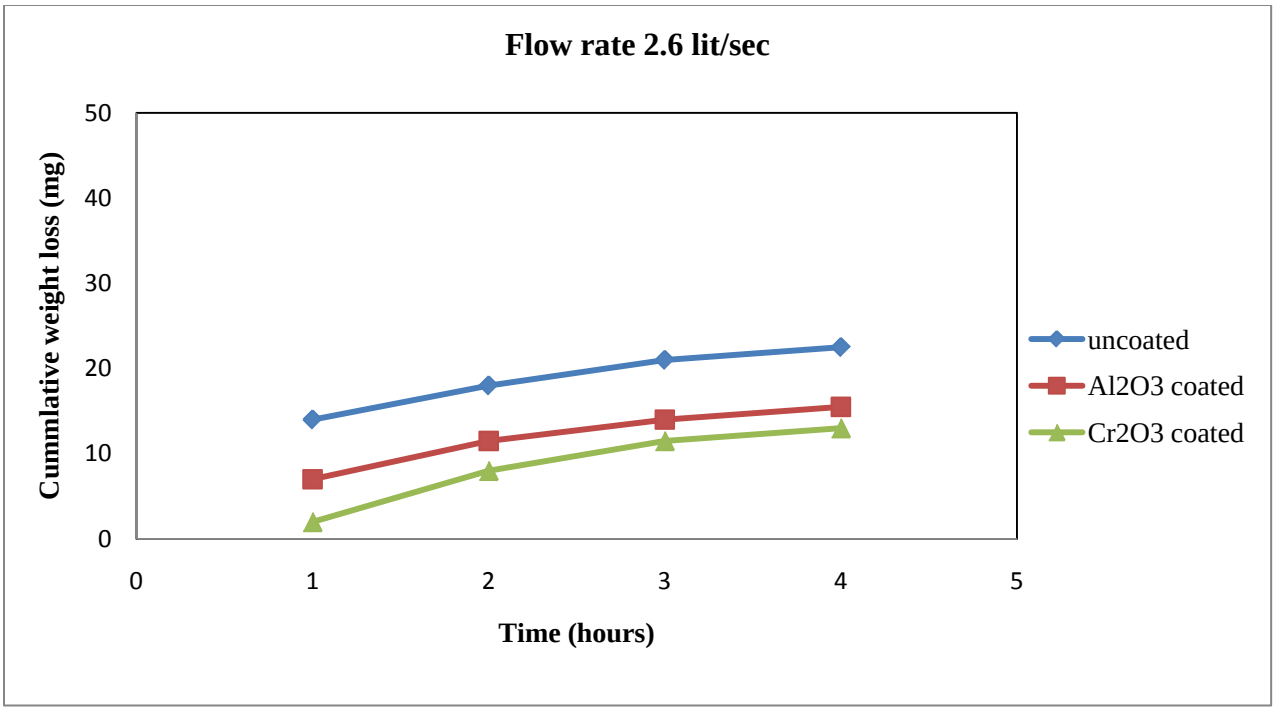

Figure 6.12 Variation in cumulative weight loss with respect to time at 90° impact angle

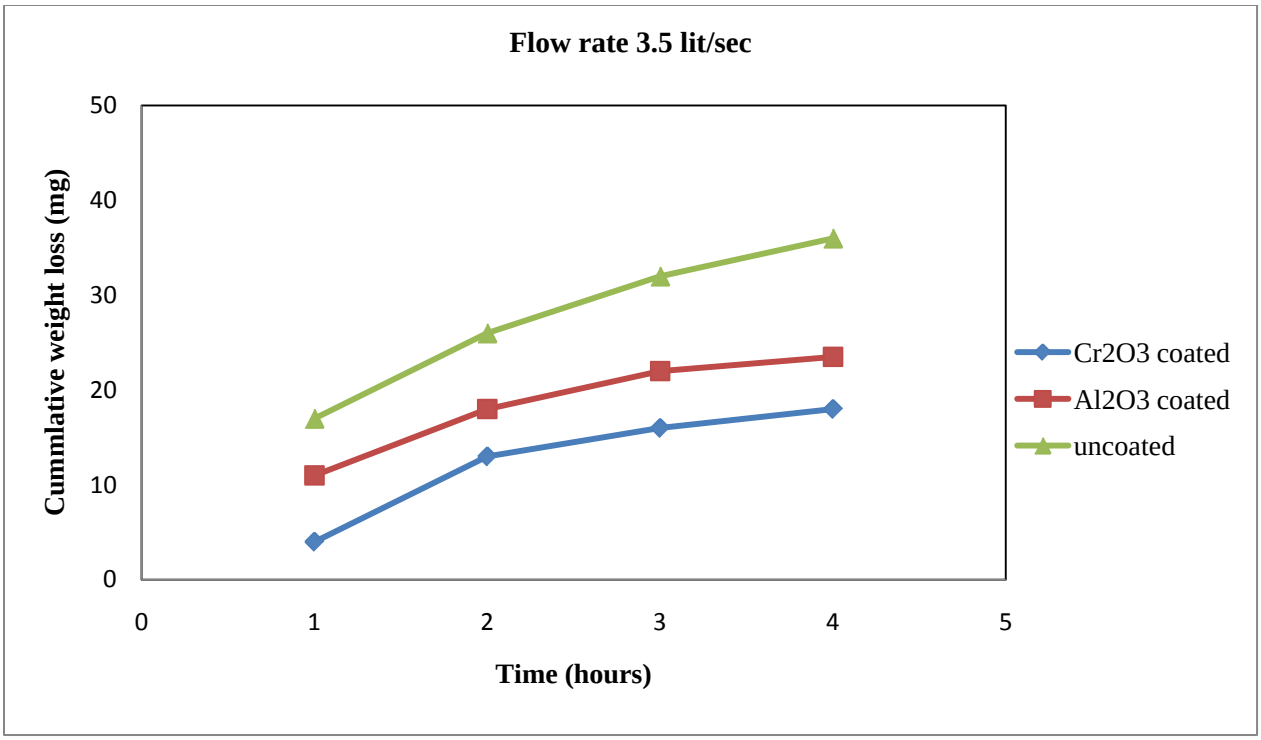

Figure 6.13 Variation in cumulative weight loss with respect to time at 90° impact angle

6.3) EFFECT OF FLOW RATE ON EROSION WEAR:

To study the effect of flow rate on erosion wear of 13Cr4Ni steel and same with coatings of aluminium oxide and cheromium oxide the wear tests are performed at three different flow rates 1.75 lit/sec, 2.6 lit/sec and 3.5 lit/sec. These observations was taken at 90° impact angle and tests duration was 3 hours.

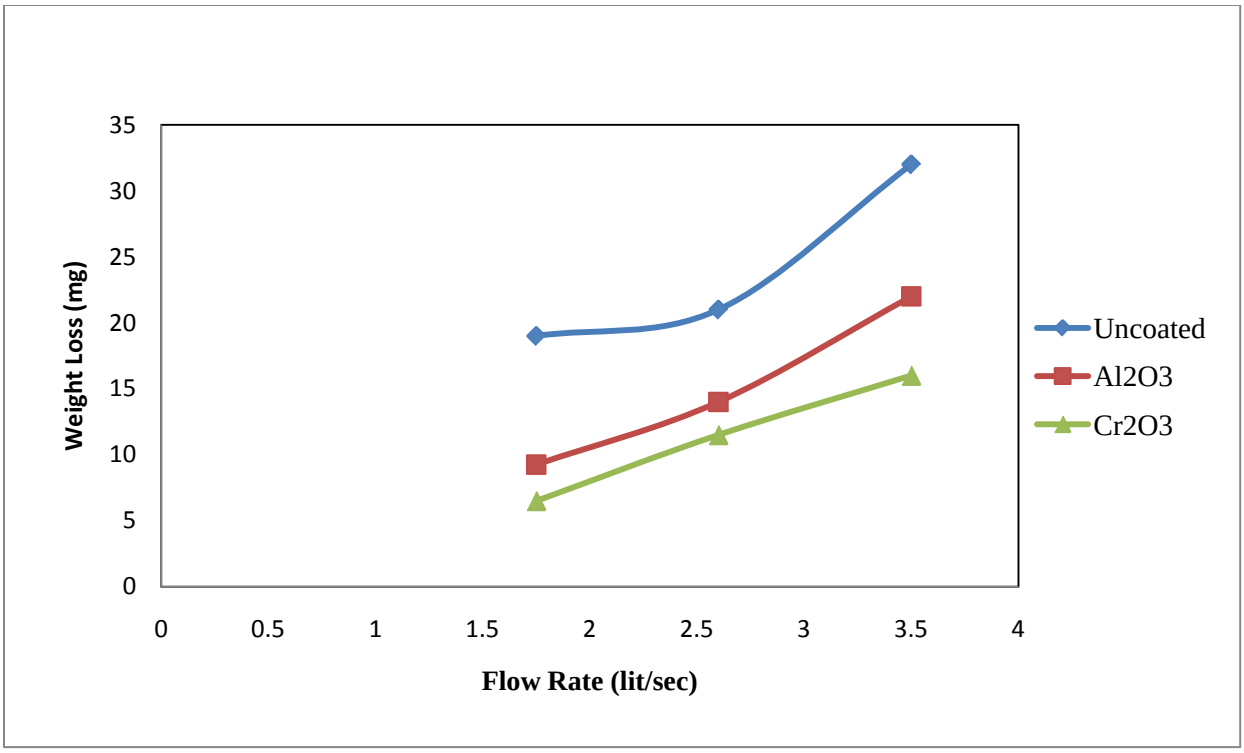

Figure 6.14 Variation in weight loss with respect to flow rate at 90° impact angle.

The effect of flow rate is be calculated by measuring the weight loss at each level of flow rate. Figure 6.14 and table 1.10 in annexure IV shows the effect of increase in flow rate on weight loss and comparison of effect of flow rate on coated and uncoated steel. From it is clear that with the increase in flow rate erosion wear also increases. The weight loss increases with increase in flow rate is because of the increase in impingement velocity of solid particles of slurry and hence kinetic energy of impacting particles increases. This increased kinetic energy of ash particles imparted to target surface and results in higher deformation and weight loss. The curve of uncoated steel shows a slite increase in weight loss initially but a larger weight loss is reported after a flow rate of 2.6 lit/sec. The erosion of coatings takes place by fatigue mechanism leading to micro cracks. The high kinetic energy of solid particles of slurry causes the cracks and with repetitive action, the fracture of coatings takes place with advancing of these cracks. Both coating clearly shows better erosion wear resistance than 13Cr4Ni steel at all different levels of flow rates. Among the both coating, chromium oxide coating shows better resistance to erosion wear than aluminium oxide coating.

6.4) EFFECT OF TIME ON EROSION WEAR:

The effect of time on erosion wear is determined by calculating the cumulative weight loss of specimen. To understand the effect of time on erosion wear, a graph (figure 6.15) is plotted between cumulative weight loss and time at a flow rate of 3.5 lit/sec. The erosion wear test duration was up to 4 hours and impact angle was 90°. It can be clearly seen in graph that amount of material loss increase with time. It slope of graphs is almost same throughout the run. It shows that the nearly equal amount of weight get lost in each interval of time depending upon the controlling parameters.

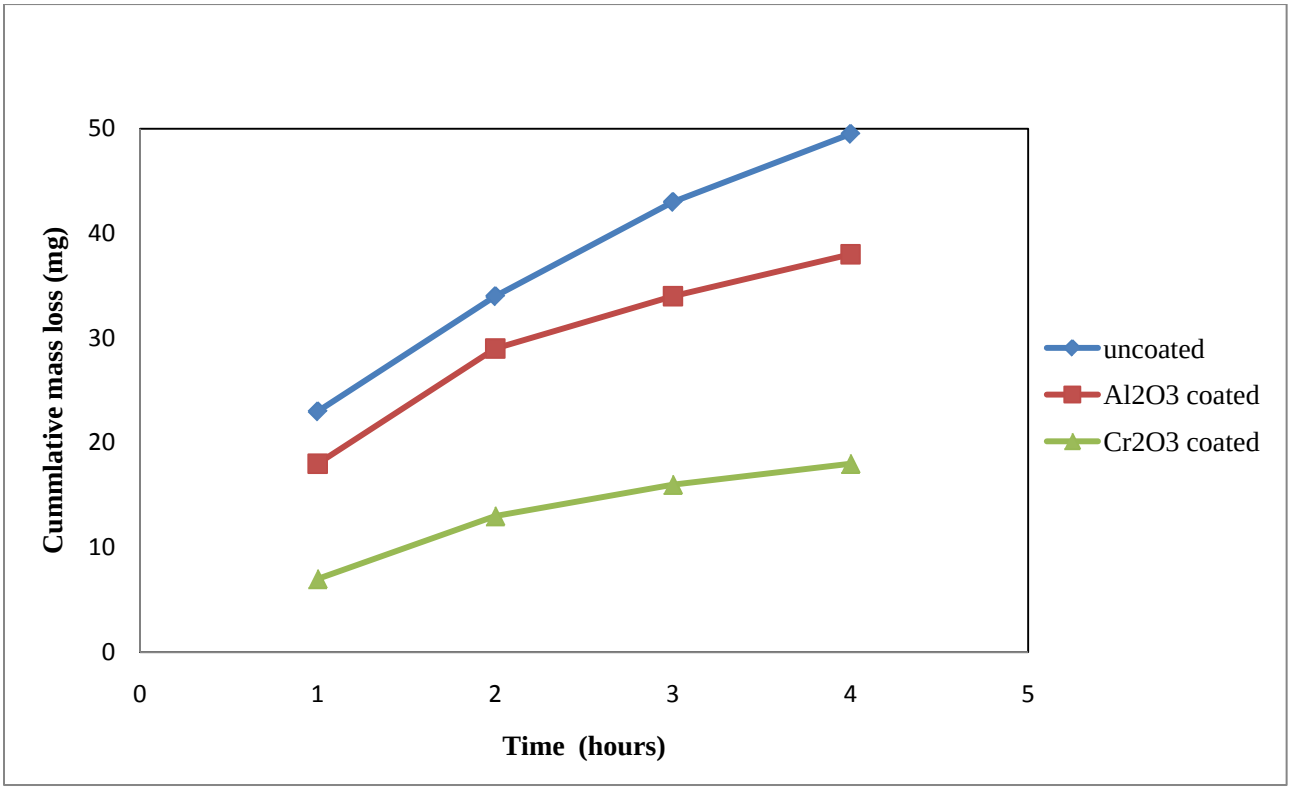

Figure 6.15 Variation in weight loss with respect to time.

The weight loss of uncoated steel is nearly equal in all time intervals and show maximum weight loss. Both coatings shows higher wear initially intervals and then reduction in wear in lateral time intervals. Chromium oxide coating shows a superior erosion wear resistance than both aluminum oxide coated and uncoated steels.

CHAPTER 7

CONCLUSION

Wear is one of the most common problems encountered in industries like thermal power plants, hydropower plants, mining industries, food-processing industries etc. in which solid liquid mixture is transported through pumps and pipes. The base material 13Cr4Ni steel taken for the

study of erosion wear of pump and piping system. To improve the wear resistance of 13Cr4Ni steel , aluminium oxide and chromium oxide powder coatings are done by HVOF thermal spray coating method. The erosion wear evaluated with varying the parameters impact angle, flow rate and time and using jet tester as test apparatus. Weight loss of specimens is the measure of erosion wear. The conclusions of the experimental work are listed below:

- Coatings of aluminium oxide and chromium oxide by HVOF method are possible on 13Cr4Ni steel.
- Both coatings shows better performance than uncoated steel in all conditions in which erosion wear test was performed.
- Chromium oxide coating shows the minimum wear as among the other aluminium oxide coating and uncoated 13Cr4Ni steel.
- Maximum erosion wear was reported at 30° impact angle and minimum at 90°.
- Cr_2O3 coated steel shows approximately 3 times better performance than uncoated 13Cr4Ni steel.
- Erosion wear rate with coating is observed that higher in initial running hours and reduces with respect to time.
- The erosion of uncoated steel under normal impact is due to platelet mechanism but for coatings under similar condition is due to crack formation.
- Erosion wear increases with increase in flow rate and test time duration.

FUTURE SCOPE

- The erosion wear studies can be performed with other coating techniques.
- The computational approach can be used to simulate the similar work with different operating conditions.

- The similar erosion wear studies can be extended by using other types of pot tester and different slurry concentration.

REFERENCES

[1] Ahmed Elkholy, “Prediction of abrasion wear slurry pump materials”. Wear 84(1983) 39-49.

[2] J. B. Zu, I. M. Ihtchings and G. T. Burstein," Design of a slurry erosion test rig", Wear, 140 (1990) 331-344.

[3] B.K. Prasad, Op Modi A.K. Jha A.K. Patwardhan, "Effects of some material and experimental variables on the slurry wear charcterstics of zinc aluminium alloy", ASM International, 1999.

[4] Gandhi BK, V. Seshadri, "Study of parametric dependence of erosion wear for the parallel flow of solid- liquid mixtures", Tribology international 32(1999) 275-282.

[5] O.P. Modi, Rupa Dasgupta, B.K. Prasad, A.K. Jha, A.H. Yegneswaran, and G. Dixit, "Erosion of high carbon steel in coal and bottom- ash slurries", Volume 9(5) Octuber 2000, Journal of Materials Engineering and performance.

[6] Craig I. Walker, Greg C. Bodkin, "Empirical wear relationships for centrifugal slurry pumps Part 1: side-liners", Wear 242(2000) 140-146.

[7] O'Flynn, D. J., Bingley, M. S., Bradley, M. S. A., and Burnett, A. J., (2001), "A model to predict the solid particle erosion rate of metals and its assessment using heat-treated steels", Wear, 248, 162-177.

[8] Craig I. Walker, "Slurry pump side- liner wear: comparison of some laboratory and field results", Wear 250 (2001) 81-87.

[9] Gandhi BK, Singh S.N, Seshadri V, "Variation of Wear along the Volute Casing of a Centrfugal Slurry Pump", JSME international Journal(2001) Vol. 44, No. 2.

[10] S.N. Singh, Gandhi BK, "Study on the effect of surface orientation on erosion wear of flat specimens moving in a solid-liquid suspension", Wear 254(2003) 1233-1238.

[11] Satish V. Borse , Gandhi BK, "Nominal particle size of multi-sized particulate slurries for evaluation of erosion wear and effect of fine particles", Wear 257(2004) 73-79.

[12] Harry H. Tian, Graeme R. Addie, "Experimental study on erosive wear of some metallic materials using Coriolis wear testing approach", Wear 258 (2005) 458–469.

[13] Kenichi Sugiyama, Shuhei Nakahama, Shuji Hattori, Keisuke Nakano, “Slurry wear and cavitation erosion of thermal-sprayed cermets”, Wear 258 (2005) 768–775.

[14] C.N. Machio, G. Akdogan, M.J. Witcomb, S. Luyckx, “Performance of WC–VC–Co thermal spray coatings in abrasion and slurry erosion tests”, Wear 258 (2005) 434–442.

[15] S. Das ,Y. S. Sarswati, D.P. Mondal, “Erosive Corrosive wear of aluminium alloy composits; influence of composition and speed”, wear 261(2006)180 – 190.

[16] G.R Desale, B.K Gandhi, S.C Jain, “Effect of erodent properties on erosion wear of ductile type materials”, Wear 261(2006) 914-921.

[17] M.C. Lin, L.S. Chang, H.C. Lin, C.H. Yang, K.M. Lin, “A study of high-speed slurry erosion of NiCrBSi thermal-sprayed coating”, Surface & Coatings Technology 201 (2006) 3193–3198.

[18] T. Manisekaran, M. Kamaraj, S.M. Sharrif, and S.V. Joshi, “Slurry Erosion Studies on Surface Modified 13Cr-4Ni Steels: Effect of Angle of Impingement and Particle Size “,ASM International (2006) 1059-9495.

[19] M.N. Noui-Mehidi , L.J.W. Graham, J. Wu, B.V. Nguyen, S. Smith, “Study of erosion behavior of paint layers for multilayer paint technique applications in slurry erosion”, Wear 264 (2008) 737–743.

[20] Y. A. Khalid and S.M. Sapuan, “Wear analysis of centrifugal slurry pump impellers”, Industrial Lubrication and Tribology 59/1 (2007) 18-28.

[21] Abel Andre C. Recco, Diana Lopez, Andre F. Bevilacqua, Felipe da Silva, Andre P. Tschiptschin, “Improvement of the slurry erosion resistance of an austenitic stainless steel with combinations of surface treatments Nitriding and TiN coating”, Surface & Coatings Technology 202 (2007) 993–997.

[22] Desale GR, Gandhi BK, Jain SC, “Slurry erosion of ductile materials under normal impact condition”, Wear 264(2008) 322-330.

[23] Narendra M. Dube, Anirudh Dube, Deepak H. Veeregowda, Suman B. Iyer; “Experimental technique to analyse the slurry erosion wear due to turbulence”, Wear 267 (2009) 259–263.

[24] J.F. Santa, L.A. Espitia, J.A. Blanco, S.A. Romo, A. Toro, “Slurry and cavitation erosion resistance of thermal spray coatings, Wear 267 (2009) 160–167.

[25] Jain SC, Gandhi BK, Desale GR, (AA 6063), “Particle size effects on the slurry erosion of aluminium alloy”, Wear 266 (2009) 1066-1071.

[26] Zhou Guanghong,Ding Hongyan, ZhangYue,LiNianlian, “Corrosion–erosion wear behaviours of 13Cr24Mn0.44N stainless steel in saline–sand slurry”. Tribology International 43 (2009) 891–896.

[27] M.M. Stack , T.M. Abd El-Badia, “Some comments on mapping the combined effects of slurry concentration, impact velocity and electrochemical potential on the erosion–corrosion of WC/Co–Cr coatings ”,Wear 264 (2008) 826–837.

[28] Y. Iwai, T. Miyajima, A. Mizuno, T. Honda, T. Itou, S. Hogmark, “Micro-Slurry-jet Erosion (MSE) testing of CVD TiC/TiN and TiC coatings ”, Wear 267 (2009) 264–269.

[29] R.C. SHIVAMURTHY, M. KAMARAJ, R. NAGARAJAN, S.M. SHARIFF, and G. PADMANABHAM, “Slurry Erosion Characteristics and Erosive Wear Mechanisms of Co-Based and Ni-Based Coatings Formed by Laser Surface Alloying ”, 470—VOLUME 41A, FEBRUARY 2010, The Minerals, Metals & Materials Society and ASM International,

[30] M. Hadad, R. Hitzek, P. Buergler, L. Rohr, S. Siegmann, “Wear performance of sandwich structured WC–Co–Cr thermally sprayed coatings using different intermediate layers”, Wear 263 (2007) 691–699, 2007 Elsevier publications.

[31] S.C.Mishra, S.Praharaj, AlokSatpathy, 2009,Evaluation of erosion wear of a ceramic coating with Taguchi approach.Journal of Manufacturing Engineering, Vol.4, Issue.2

[32] B.S. Mann, VivekArya, A.K. Maiti, M.U.B. Rao and Pankaj Joshi, 2006, Corrosion and erosion performance of HVOF/TiAlN PVD coatings and candidate material for high pressure gate valve application.Wear, 75-82

[33] A. Neville, F. Reza, S. Chiovelli, T. Revegab, 2005, Erosion–corrosion behaviour of WC-based MMCs in liquid–solid slurries. Wear, 181–195.

[34] Factor M., Roman I., 2002,Microhardness as a simple means of estimating relative wear resistance of carbide thermal spray coatings**.**Journal of thermal spray technology, 482-495

ANNEXURE I

Table 1.1 Particle size distribution of Fly ash

SAMPLE SIZE: 250 GM							
READING IN GRAMS							
S.NO	SIZE RANGE(IN MICRONS)below	Average % Fly Ash	% Finer Fly Ash	Xi Fly	Wi Fly	WiXi Fly	Dwmi Fly
1				0	0	0	
2				0	0	0	
3		0.0052		-355	1.3	-461.5	
4	355	0.0052	100.00%	55	1.3	71.5	
5	300	0.0072	99.00%	50	1.8	90	
6	250	0.01	98.50%	38	2.5	95	**19**
7	212	0.004	97.00%	32	1	32	
8	180	0.09	95.00%	30	22.5	675	
9	150	0.0332	92.00%	25	8.3	207.5	
11	125	0.034	88.00%	35	8.5	297.5	
12	90	0.46	80.00%	15	115	1725	
13	75	0.307	69.00%	22	87.8	1931.6	
	53		48%		250	4663.6	

ANNEXURE II

Table 1.2 Static settled Concentration of fly ash

Time(Min)	Concentration.(%Cw)
0	20
1	24.97
2	25.28
3	29.8
4	32.2
5	44.35
15	53.9
30	54.49
60	55.7
120	55.7
180	56.98
240	56.98
480	56.98

Table 1.3 Shear Stress- Shear rate of fly ash slurry at different concentrations

Concentration →	10%	20%	30%	40%	50%
Shear Stress, Shear Rate ↓					
0	0	0	0	0	0
50	0.065	0.085	0.11	0.41	1
75	0.0975	0.15	0.165	0.6875	1.11
100	0.16	0.17	0.26	0.79	1.19
125	0.17	0.24	0.28	0.88	1.2875
150	0.2	0.255	0.39	0.925	1.385
175	0.24	0.2975	0.53	0.97	1.5225
200	0.29	0.39	0.49	1.08	1.74
225	0.3	0.3825	0.58	1.28	1.9575

ANNEXURE III

Table 1.4 Concentration Vs relative viscosity of fly ash slurry:

Concentration (% age wt.)	Relative Viscosity
0	1
10	2.11
20	3.42
30	3.92
40	6.89

Table 1.5 Concentration Vs pH value of fly ash slurry:

Concentration (% age wt.)	pH
0	7.75
10	7.61
20	7.59
25.9	7.55
30	7.51
35	7.48
40	7.46
45	7.45
50	7.44

ANNEXURE IV

Table 1.6 Variation in weight loss with respect to impact angle at 1.75 lit/sec flow rate and 3 hour test time duration.

	WEIGHT LOSS IN MILLIGRAMS		
Impact Angle	Uncoated 13Cr4Ni Steel	Al_2O_3 Coated Steel	Cr_2O_3 Coated Steel
30°	33	18.5	9
60°	24	10.5	7
90°	19	9.25	6.5

Table 1.7 Variation in weight loss with respect to time and impact angle at 1.75 lit/sec slurry flow rate.

TIME (in hours)	WEIGHT LOSS IN MILLIGRAMS								
	At Impact Angle 30°			At Impact Angle 60°			At Impact Angle 90°		
	Uncoated Steel	Al_2O_3 Coated	Cr_2O_3 Coated	Uncoated Steel	Al_2O_3 Coated	Cr_2O_3 Coated	Uncoated Steel	Al_2O_3 Coated	Cr_2O_3 Coated
1	22	11	3.5	12	6	2	8	4	1.5
2	29	16	7.5	21	9	5.5	15	8.5	3
3	33	18.5	9	24	10.5	7	19	9.25	6.5
4	37.5	20	10.5	26	12	8.5	21	11	8.5

Table 1.8 Variation in weight loss with respect to time and impact angle at 2.6 lit/sec slurry flow rate.

TIME (in hours)	WEIGHT LOSS IN MILLIGRAMS								
	At Impact Angle 30°			At Impact Angle 60°			At Impact Angle 90°		
	Uncoated Steel	Al_2O_3 Coated	Cr_2O_3 Coated	Uncoated Steel	Al_2O_3 Coated	Cr_2O_3 Coated	Uncoated Steel	Al_2O_3 Coated	Cr_2O_3 Coated
1	28	13	6	19	11	4	14	7	2
2	31	17.5	9	27	14.5	9	18	11.5	8
3	36	19	13	36	17	12	21	14	11.5
4	40	22	15	41	19	14	22.5	15.5	13

Table 1.9 Variation in weight loss with respect to time and impact angle at 3.5 lit/sec slurry flow rate.

TIME (in hours)	WEIGHT LOSS IN MILLIGRAMS								
	At Impact Angle 30°			At Impact Angle 60°			At Impact Angle 90°		
	Uncoated Steel	Al_2O_3 Coated	Cr_2O_3 Coated	Uncoated Steel	Al_2O_3 Coated	Cr_2O_3 Coated	Uncoated Steel	Al_2O_3 Coated	Cr_2O_3 Coated
1	32	19.5	8.5	23	18	7	17	11	4
2	35	26	14	34	29	13	26	18	13
3	36.5	31	16.5	43	34	16	32	22	16
4	43	36.5	19	49.5	38	18	36	23.5	18

Table 1.10 Variation in weight loss with respect to flow rates at 90° impact angle and 3 hour test time duration.

	WEIGHT LOSS IN MILLIGRAMS		
Flow Rate	**Uncoated 13Cr4Ni Steel**	**Al_2O_3 Coated Steel**	**Cr_2O_3 Coated Steel**
1.75	19	9.25	6.5
2.6	21	14	11.5
3.5	32	22	16